

Organic geochemistry of the Woodford Shale, southeastern Oklahoma: How variable can shales be?

Andrea Miceli Romero and R. Paul Philp

ABSTRACT

Woodford Shale samples, obtained from a cored outcrop in southeastern Oklahoma, were geochemically analyzed to determine vertical variations of organic facies, thermal maturity, and an evaluation of their depositional environments. Total organic carbon values ranged from 5.01 to 14.81%, indicating a good source rock potential. In this area, the Woodford Shale is marginally mature, as indicated by vitrinite reflectance values. Rock-Eval data revealed that the samples are dominated by type II kerogen. Biomarker ratios, based on pristane, phytane, steranes, and hopanes, show a mix of marine and terrigenous organic matter. High-salinity conditions and water density stratification also prevailed during deposition of this formation, as indicated by the presence of gammacerane.

The Woodford Shale was subdivided into lower, middle, and upper members based on the integration of geochemical and geologic data. Moreover, the presence and extent of photic zone anoxia (PZA) were determined by the presence of aryl isoprenoids. The lower and upper Woodford Shale members were deposited under dysoxic to suboxic conditions and episodic periods of PZA. The middle member was deposited under anoxic conditions and persistent PZA. In addition, aryl isoprenoids helped infer the position of the chemocline during deposition of the different members. The relative hydrocarbon potential parameter was used in determining transgressive and regressive cycles within the Woodford Shale.

This study undoubtedly demonstrates the significant lithologic and chemical variability that occurs within shales. The application of this workflow to regional studies can have a

AUTHORS

ANDREA MICELI ROMERO ~ University of Oklahoma, ConocoPhillips School of Geology and Geophysics, Norman, Oklahoma 73019; andreamiceli@ou.edu

Andrea Miceli Romero is a Ph.D. student at the University of Oklahoma. She obtained her B.Sc. degree in geochemistry from Universidad Central de Venezuela in 2006 and her M.Sc. degree in geology from the University of Oklahoma in 2010. Her interests include geochemical characterization of source rocks and hydrocarbons from unconventional reservoirs, with emphasis in biomarkers.

R. PAUL PHILP ~ University of Oklahoma, ConocoPhillips School of Geology and Geophysics, Norman, Oklahoma 73019; pphilp@ou.edu

R. Paul Philp obtained his B.Sc. degree in chemistry from the University of Aberdeen in 1968 and his Ph.D. and D.Sc. degree from the University of Sydney in 1972 and 1998, respectively. He is currently a geochemistry professor at the University of Oklahoma. His interests include geochemical characterization of unconventional gas shales, characterization of novel biomarkers and high-molecular-weight hydrocarbons, and use of stable isotopes in environmental problems.

ACKNOWLEDGEMENTS

The authors extend their gratitude to the School of Geology and Geophysics at the University of Oklahoma, Devon Energy, and to the AAPG Grants-In-Aid Foundation for providing the financial support to this research. We thank Roger M. Slatt, Brian J. Cardott, and Erik P. Kvale for their valuable comments and suggestions for this article. Special thanks to Brian J. Cardott for the vitrinite reflectance measurements. Thanks to T. Nichole Buckner for sharing some of her data to support some of the results presented here and to the OU-Devon-Schlumberger Project for providing the core samples. The authors thank the reviewers for their corrections and suggestions. The AAPG Editor thanks the following reviewers for their work on this paper: Karen S. Glaser, Richard B. Koepnick, and Fang Lin.

Copyright ©2012. The American Association of Petroleum Geologists. All rights reserved.

Manuscript received January 31, 2011; provisional acceptance April 19, 2011; revised manuscript received July 11, 2011; final acceptance August 10, 2011.

DOI:10.1306/08101110194

direct influence on exploration and production activities in shale-gas systems.

INTRODUCTION

The Woodford Shale (Upper Devonian–Lower Mississippian), once only considered as a source rock for oil and natural gas in the southern mid-continent, has recently evolved as an important shale gas play because of its high hydrocarbon potential. In south-central and southeastern Oklahoma, this formation mainly yields gas and, to a lesser extent, oil (Cardott, 2005; Comer, 2007).

Considering shales as uniform stratigraphic sequences in terms of physical and chemical properties is common. However, it has been demonstrated that a more detailed analysis of this source and now also reservoir rocks can provide greater insights about variations in the depositional and environmental factors that influenced its deposition (Hester et al., 1990; Hickey and Henk, 2007; Loucks and Ruppel, 2007; Singh, 2008; Comer, 2009; Slatt et al., 2009a, b, c, d).

Moreover, industry and academia have worked together to evaluate shale gas characteristics (e.g., shale type, organic content, porosity, permeability, maturity, frac-ability, gas content, reservoir thickness, and volumetrics, among others) with the aim of defining sweet spots, gas fairways, or producible areas of economic potential (Schmoker, 2002; Jarvie et al., 2005, 2007; Schenk, 2005; Boyer et al., 2006; Gale et al., 2007; Pollastro, 2007). In this regard, geochemistry is an important factor in shale gas evaluation. Different approaches and techniques have been used to determine maturity and organic content of shales: organic matter type, quantity and provenance, thermal maturity, type of hydrocarbons generated, the function of clay minerals in concentrating organic matter within the reservoirs, depositional settings, and burial history modeling. This information has been integrated with information from other disciplines such as geology, geophysics, reservoir engineering, and petroleum engineering to determine shale gas potential and attempt to define petroleum systems for these types of plays (Curtis, 2002; Jarvie et al., 2005, 2007; Hill

et al., 2007a, b; Philp, 2007; Pollastro et al., 2007; Zhao et al., 2007; Kinley et al., 2008; U.S. Geological Survey, 2009).

The main objective of this study is to geochemically characterize the Woodford Shale in terms of organic richness, organic matter type, hydrocarbon generation potential and thermal maturity, variations in organic matter sources, and depositional environments, which are linked to the geology and sequence stratigraphy of this play in southeastern Oklahoma.

REGIONAL GEOLOGY

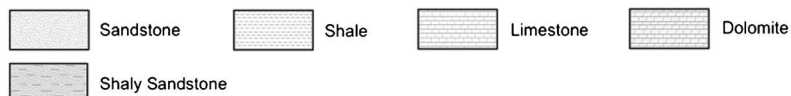
The Woodford Shale is an organic-rich black shale characterized by the presence of chert, siltstone, sandstone, dolostone, and light-colored shale. In addition, laminations of reddish-brown clay and organic matter with scattered siliceous spheres, lenses, and opaque minerals can be found. Phosphate nodules, pyrite concretions, and calcite concretions are early diagenetic products and related to oxidation of organic matter by anaerobic organisms (Kirkland et al., 1992; Comer, 2007). The basal sediments of the Woodford Shale correspond to the Misener-Sylamore Sandstones. The Woodford unconformably overlies the limestones and dolomites of the Hunton Group (Silurian–Devonian). In the Arkoma Basin, the Caney Shale conformably overlies the Woodford Shale (Figure 1) (Ham, 1973; Sullivan, 1985; Northcutt et al., 2001; Portas, 2009).

Kirkland et al. (1992) considered several factors that could have contributed to the preservation of organic matter within the Woodford Shale. One of the most important was the establishment of anoxic bottom-water conditions that inhibited the activity of aerobic microorganisms. Under these conditions, the algal organic matter is resistant to bacterial degradation. These factors, combined with a slow sedimentation rate, generated organic-rich source rocks during the Late Devonian.

Several authors have divided the Woodford Shale into different informal stratigraphic units based on lithology and well responses (Ellison, 1950), palynomorph distributions (Urban, 1960),

AGE		STRATIGRAPHIC UNIT		
SYSTEM \ SERIES		ARKOMA BASIN		
		Formation	Lithology	Depositional Environment
PENNSYLVANIAN	DESMOINES	Boggy Formation Hartshorne Sandstone		Fluvial-Deltaic
	ATOKA	Atoka Formation Spiro Sandstone		Channel and Bar
	MORROW	Wapanucka Limestone Game Refuge Sandstone		Shallow-Marine Channel and Bar
MISSISSIPPIAN		Springer Group Caney Shale		Deep Marine
DEVONIAN		Woodford Shale Misener Sandstone		Deep Marine
SILURIAN		Hunton Group		Shallow Marine
ORDOVICIAN		Sylvan Shale Viola Limestone Simpson Group Arbuckle Group		Shallow Marine Shallow Marine
CAMBRIAN		Honey Creek Formation Reagen Sandstone		Shallow Marine
PRECAMBRIAN		Metamorphic Rocks		

Vertical dots indicate that numerous stratigraphic unit names were omitted.



geochemistry (Sullivan, 1985), log character and kerogen content (Hester et al., 1990), and gamma-ray logs (Krystyniak, 2003; Paxton et al., 2007). The subdivision of upper, middle, and lower Woodford Shale members presented in this work is broadly similar to these previously proposed zonation schemes.

SAMPLES AND METHODS

The Wyche 1 well was drilled, cored, and logged behind an active quarry in the Wyche shale pit, Pon-

Figure 1. Stratigraphic chart for the Arkoma Basin, southeastern Oklahoma (modified from Portas, 2009).

toc County, as part of a University of Oklahoma–Devon–Schlumberger project. The walls within the quarry reach more than 50 ft (>16 m), exposing the Woodford Shale in three dimensions (Figure 2). The core is 200 ft (61 m) long, but the basal contact of the Woodford Shale with the Hunton Limestone can only be observed in the suite of logs that were run for this well (Figure 3) (Portas, 2009). A total of 20 core samples were selected according to the intervals of interest on a simultaneous stratigraphic study. The samples were subjected to several geochemical analyses, including Rock-Eval pyrolysis, total organic carbon (TOC), and vitrinite reflectance (R_o). In addition, crushed rock extracts

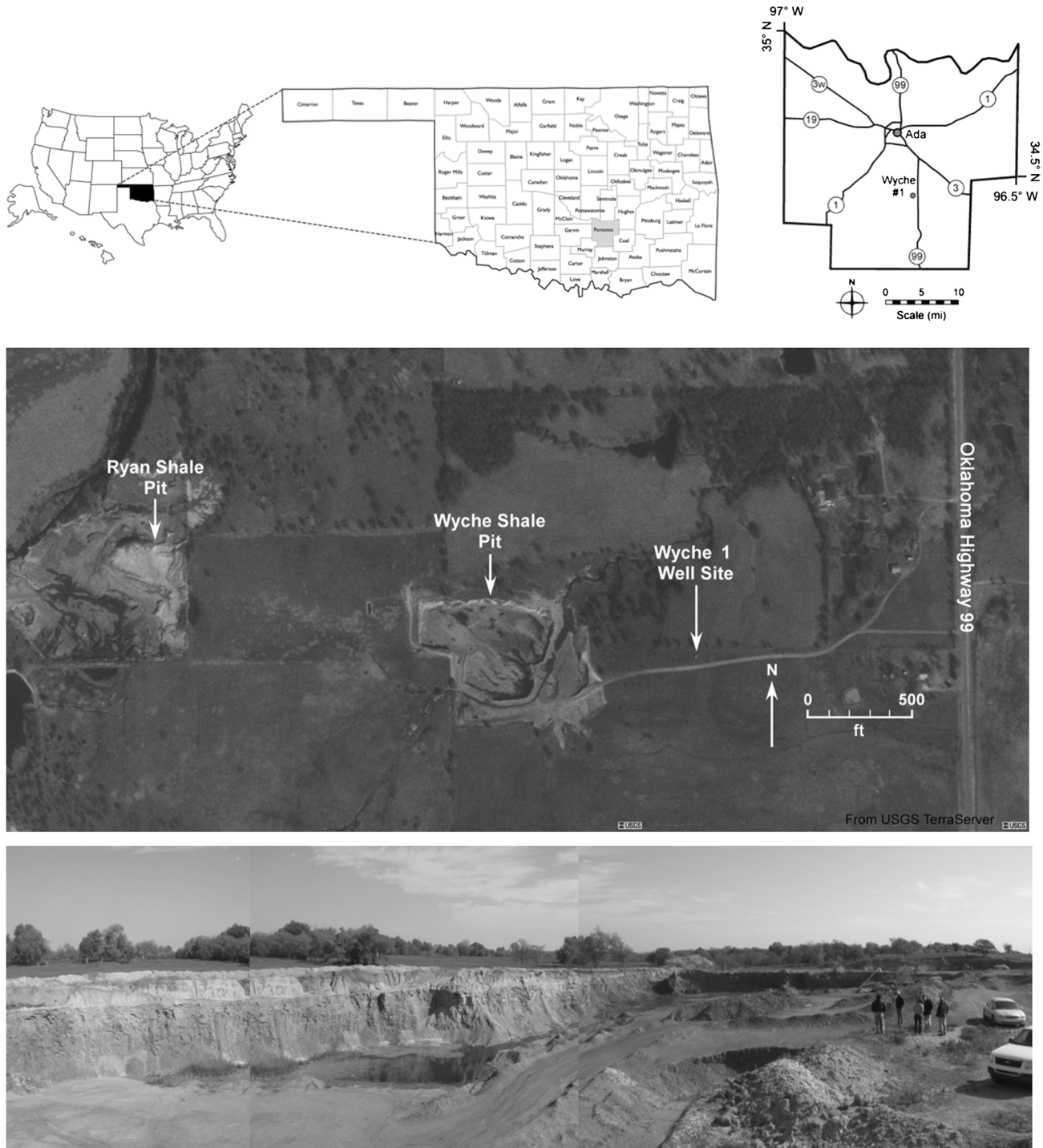


Figure 2. Map and images showing the location of the Wyche shale pit and the Wyche 1 well site (photographs courtesy of T. Nichole Buckner).

were subjected to gas chromatography (GC) and gas chromatography–mass spectrometry (GC-MS) for biomarker analyses. A list of all the Woodford Shale samples analyzed is presented in Table 1.

A summary of the laboratory techniques used in this project is depicted in Figure 4. Details of the experimental procedures are presented in the Appendix.

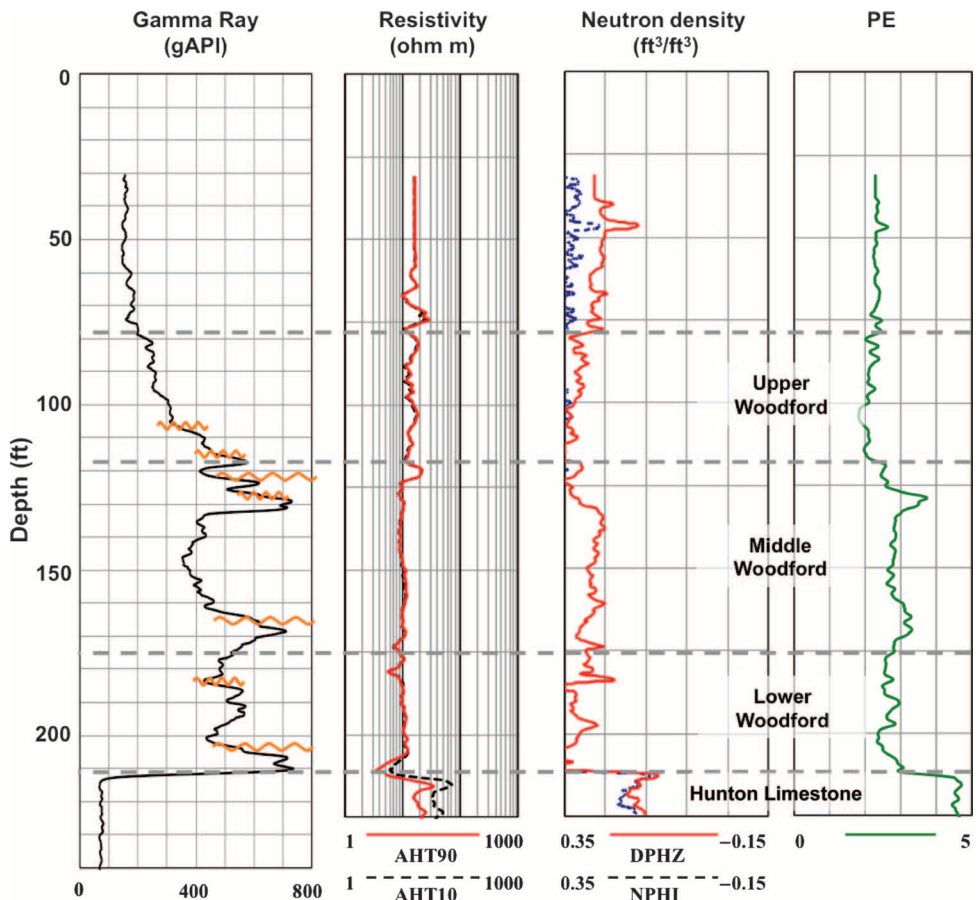


Figure 3. Gamma-ray, resistivity, neutron density, and photoelectric (PE) factor logs for the Wyche 1 well (Buckner et al., 2009). Subdivision of the Woodford Shale members is based on analysis of geologic and geochemical data. Squiggles represent unconformities. ATH = array induction two-foot resistivity (numbers indicate depth of penetration in feet); DPHZ = standard resolution density porosity; NPHI = thermal neutron porosity.

RESULTS AND DISCUSSION

Source Rock Characterization

Total organic carbon values range between 5.01 and 14.81%, with the minimum value observed at a depth about 160 ft (~49 m), which are indicative of very good to excellent potential source rocks (Peters, 1986; Peters and Cassa, 1994) (Table 2). Geochemical logs for the Wyche 1 well were constructed to illustrate variation of Woodford Shale TOC with depth (Figure 5). Two breaks occur at about 118 and 185 ft (~36 and 56 m), which could be attributed to a change in lithologic or mineralogical characteristics of the unit. Slatt et al. (2011) established important facies changes across these depths that were used to define the upper-middle and middle-lower Woodford Shale boundaries. In addition, Buckner et al. (2009) observed a major change in log signatures from the Wyche 1 well at about 118 ft (~36 m) primarily indicated by an

increase in gamma-ray and decrease in resistivity values (T. N. Buckner, 2010, personal communication). This change was used to determine the boundary between the upper and middle Woodford. Slatt et al. (2011) also observed variations on different electrical logs at about 175 ft (~53 m), which were attributed to the middle-lower boundary of the Woodford Shale. For the Wyche 1 well, a core-to-log correction of about 10 ft (~3 m) should be made because a depth shift occurred when the core was taken (T. N. Buckner, 2010, personal communication). The core broke at 160 ft (49 m) and separated for about 10 ft (~3 m). The core gamma scan and the rock sampling considered this gap as a missing section, not as a depth shift in the lower section of the core. However, when comparing the gamma-ray log with the core gamma scan (Figure 5), it can be observed that the gap in the log actually corresponds to a depth shift in the core. Therefore, petrophysical interpretations are consistent with the geochemical variations observed on

Table 1. List of the Woodford Shale Samples Analyzed in This Study

Sample	Depth (ft)	Woodford Shale Member
WCWF-1	92.21	Upper
WCWF-2	97.92	
WCWF-3	103.00	
WCWF-4	107.08	
WCWF-5	111.00	
WCWF-6	113.08	
WCWF-7	115.13	
WCWF-8	118.04	Middle
WCWF-9	121.17	
WCWF-10	123.13	
WCWF-11	130.41	
WCWF-12	139.15	
WCWF-13	151.08	
WCWF-14	157.83	
WCWF-15	170.45	Lower
WCWF-16	181.04	
WCWF-17	186.90	
WCWF-18	192.35	Lower
WCWF-19	198.21	
WCWF-20	208.08	

the samples from this study. In consequence, we propose that the core analyzed contains the three Woodford Shale members commonly described in

Figure 4. Schematic workflow used in the laboratory analysis. TOC = total organic carbon; CH_3OH = methanol; CH_2Cl_2 = dichloromethane; HPLC = high-performance liquid chromatography; NSO = nitrogen, sulfur, oxygen (polar) compounds or resins; GC = gas chromatography; GC-MS = gas chromatography–mass spectrometry.

the literature (Ellison, 1950; Urban, 1960; Sullivan, 1985; Hester et al., 1990; Lambert, 1993; Krystyniak, 2003; Paxton et al., 2007; Comer, 2008; Slatt et al., 2011).

A modified Van Krevelen diagram (Figure 6) shows the distribution of all the Woodford Shale samples analyzed. However, variations of this parameter within this sample set can be attributed to differences in organic facies. The upper and middle Woodford members are grouped together, possibly indicating a similar organic facies, whereas the lower member samples are more scattered. Woodford samples from the Wyche 1 well have high hydrogen index (HI) values (>300) and appear to be dominated by type II kerogen. The marine origin for the Woodford Shale is undisputable (Kirkland et al., 1992; Fritz and Beaumont, 2001; Northcutt et al., 2001), and because of its age, the input of higher plant material should have been minimal. In consequence, the high HI values obtained from the organic matter of these samples were likely caused by the predominance of marine algae, which is hydrogen rich, similar to lacustrine algae. The overall high HI and S_2/S_3 values (Table 2) indicate that the Woodford Shale samples are mainly oil prone according to the guidelines proposed by Peters (1986) and Peters and Cassa (1994).

Measured and calculated R_o values (Table 3) show that the Woodford Shale samples have a low

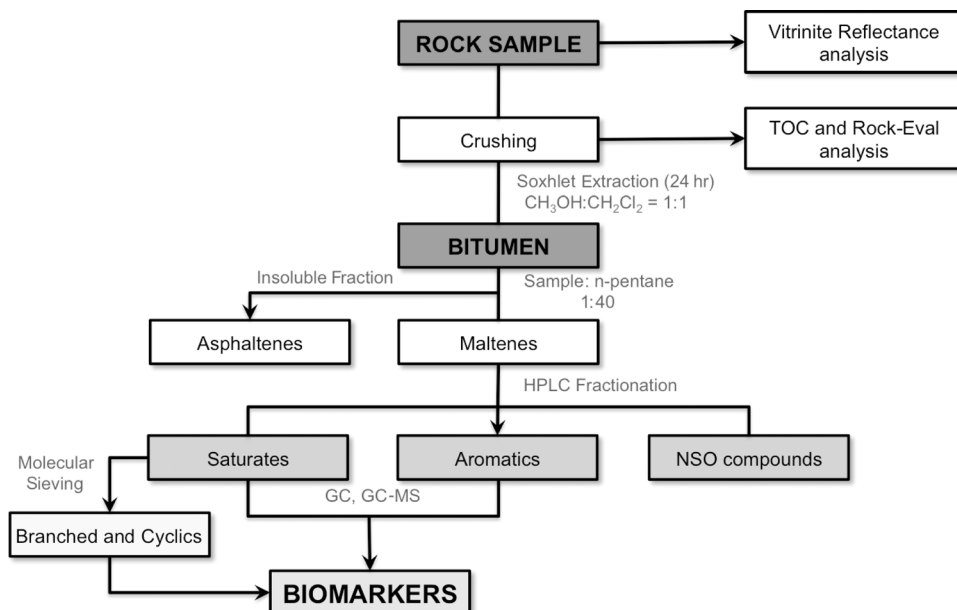


Table 2. Total Organic Carbon and Rock-Eval Data from Core, Cuttings, and Outcrop Samples Used in This Study

Woodford Shale Member	Sample No.	TOC*	S_1^* (mg HC/g rock)	S_2^* (mg HC/g rock)	S_3^* (mg CO ₂ /g rock)	T_{\max}^* (°C)	HI* (mg HC/g TOC)	OI* (mg CO ₂ /g TOC)	S_2/S_3^* (mg HC/mg CO ₂)	S_1/TOC^*	PI*
Upper	WCWF-1	5.16	1.05	33.34	0.55	433	646	11	60.62	20.00	0.03
	WCWF-2	7.09	1.38	50.50	0.56	432	712	8	90.18	19.00	0.03
	WCWF-3	8.72	2.26	61.77	0.53	431	708	6	116.55	26.00	0.04
	WCWF-4	7.44	3.03	51.51	0.50	425	692	7	103.02	41.00	0.06
	WCWF-5	8.44	2.19	59.44	0.54	424	704	6	110.07	26.00	0.04
	WCWF-6	9.82	2.14	76.60	0.49	436	780	5	156.33	22.00	0.03
	WCWF-7	9.95	2.43	69.94	0.50	427	703	5	139.88	24.00	0.03
Middle	WCWF-8	10.97	2.75	66.67	0.53	423	608	5	125.79	25.00	0.04
	WCWF-9	8.66	1.95	52.25	0.59	427	603	7	88.56	23.00	0.04
	WCWF-10	9.77	2.06	56.28	0.58	424	576	6	97.03	21.00	0.04
	WCWF-11	13.50	3.35	53.55	1.30	415	397	10	41.19	24.79	0.06
	WCWF-12	5.74	1.60	33.78	0.58	425	589	10	58.24	28.00	0.05
	WCWF-13	8.40	2.68	45.95	1.00	419	547	12	45.95	31.84	0.06
	WCWF-14	5.01	1.32	29.00	0.55	421	579	11	52.73	26.00	0.04
	WCWF-15	7.95	1.88	33.72	1.07	412	424	13	31.51	23.63	0.05
	WCWF-16	9.42	2.68	47.68	1.18	418	506	13	40.41	28.43	0.05
Lower	WCWF-17	10.61	2.59	58.91	0.93	425	555	9	63.34	24.00	0.04
	WCWF-18	8.34	2.43	37.94	1.20	416	455	14	31.62	29.15	0.06
	WCWF-19	8.23	2.69	55.90	0.75	414	679	9	74.53	33.00	0.05
	WCWF-20	14.81	4.03	95.53	1.01	421	645	7	94.58	27.00	0.04

* S_1 = free volatile hydrocarbons (HCs) thermally flushed from a rock sample at 300°C (free oil content); S_2 = products that crack during standard Rock-Eval pyrolysis temperatures (remaining potential); S_3 = organic carbon dioxide released from rock samples; T_{\max} = temperature at peak evolution of S_2 HCs; HI (hydrogen index) = $S_2 \times 100/\text{total organic carbon (TOC)}$; OI (oxygen index) = $S_3 \times 100/\text{TOC}$; S_2/S_3 = type of HCs generated; S_1/TOC = normalized oil content; PI (production index): $S_1/(S_1 + S_2)$ (or transformation ratio).

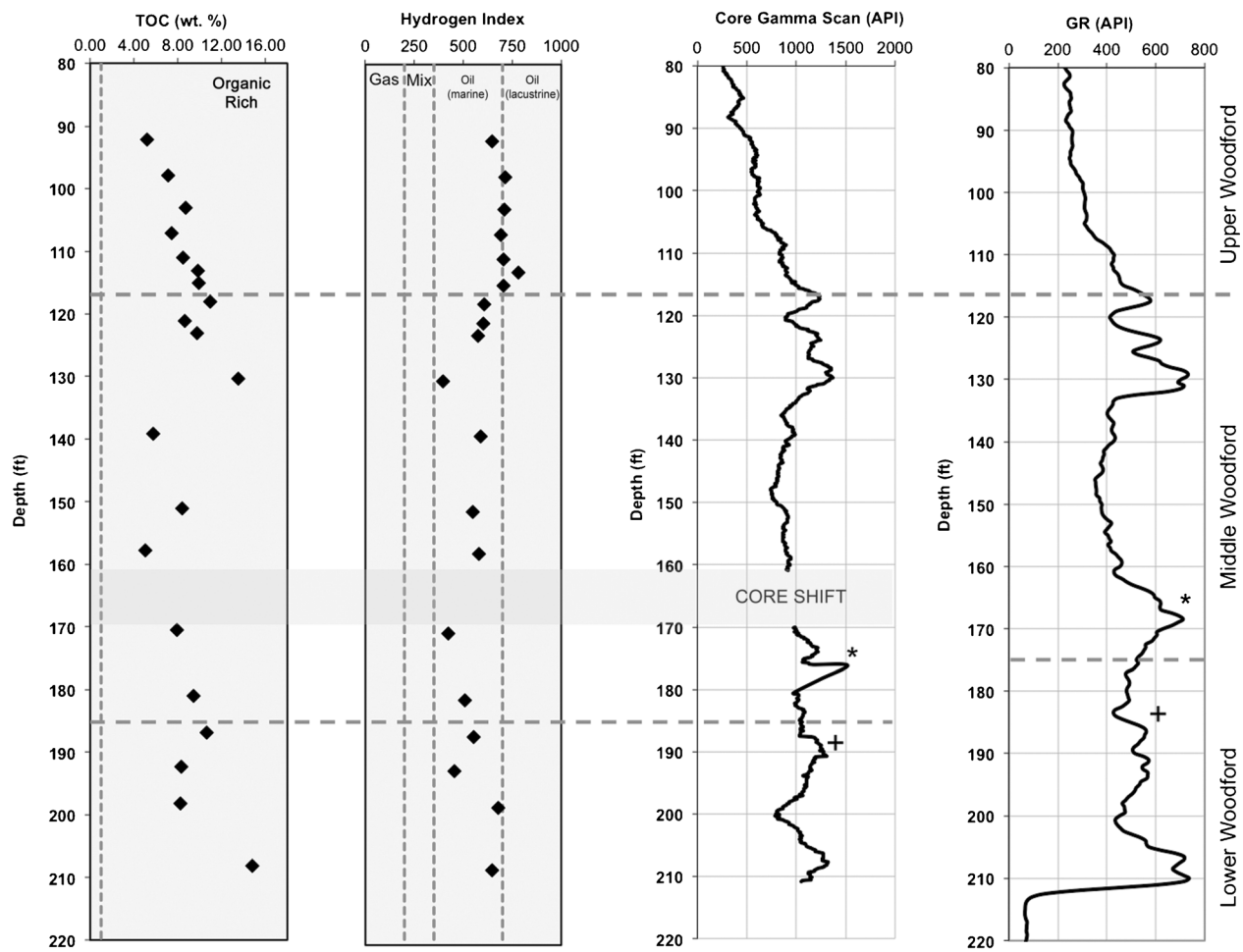


Figure 5. Geochemical log showing the total organic carbon (TOC) and hydrogen index (plot template modified from Humble Geochemical Services). Gamma-ray (GR) log and core gamma scan for the Wyche 1 well. Asterisk and cross indicate similar log patterns that confirm the approximate 10-ft (~3-m) core shift.

thermal maturity, indicating that, in this area, this formation has not yet entered the oil window. As a consequence, any Woodford Shale gas present in this area has likely been generated in association with oil.

Biomarker Analysis

Gas chromatograms for the saturate fractions of the Woodford Shale samples (Figure 7) do not show much variability. All the samples exhibit unimodal distributions of n-alkanes toward the low-carbon number members ($n\text{-C}_{24}$) and with a maximum about $n\text{-C}_{15}$, but no odd or even predominance. Because these samples are immature, the absence of odd or even predominance and the low quanti-

ties of high-molecular-weight compounds indicate a predominance of marine organic matter input. In general, phytoplankton, zooplankton, and benthic algae are the main organisms that contribute to marine organic matter showing similar n-alkane distributions (Tissot and Welte, 1978; Jones and Philp, 1990). These characteristics are comparable to previous studies on the Woodford Shale presented by Burruss and Hatch (1989), Philp et al., (1989), Jones and Philp (1990), and Wang and Philp (1997).

Pristane (Pr) and phytane (Ph) were identified on the gas chromatograms of the saturate fraction isolated from the bitumen extracts. The Pr/Ph ratios for the Woodford Shale samples range from 1.11 to 3.48 (Table 4). A geochemical log of Pr/Ph ratios for the Wyche 1 well (Figure 8) exhibits slight

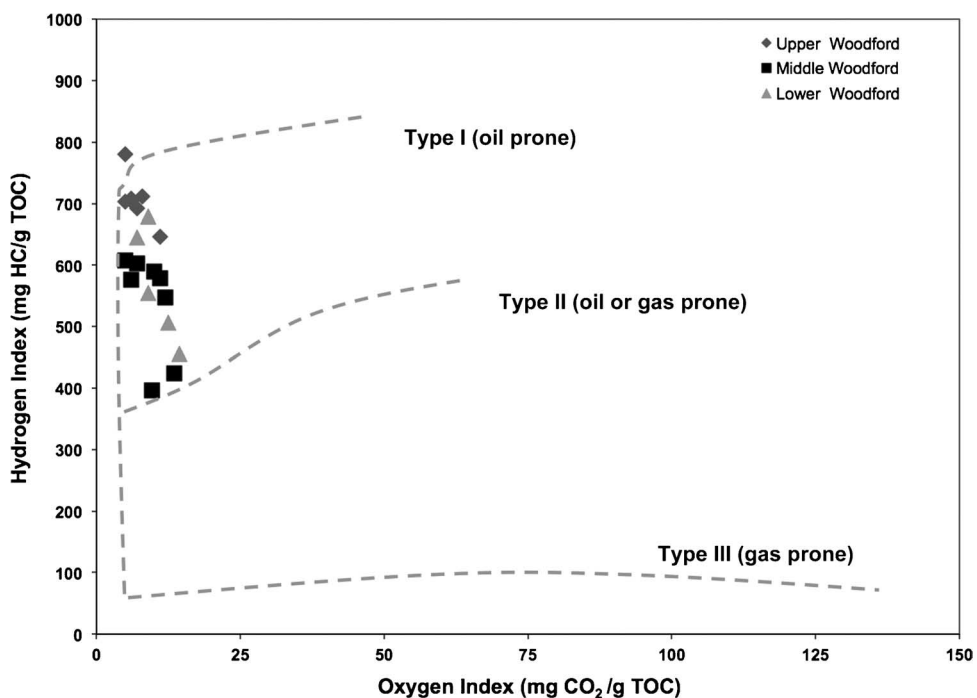


Figure 6. Modified Van Krevelen diagram for the Woodford Shale samples showing that this source rock is dominated by type II kerogen.

variations in redox conditions along the profile. However, the larger values appear at the top and bottom of the section, indicating greater oxygen content during deposition of the lower and upper Woodford Shale members. Higher Pr/Ph values at the bottom of the lower Woodford Shale member reflect more oxic conditions because of weathering and erosion associated with the well-known unconformity between the Woodford Shale and Hunton Limestone.

A diagram of Pr/n-C₁₇ versus Ph/n-C₁₈ ratios for the Woodford Shale samples is presented as Figure 9 (Hunt, 1995). Most of the samples plot along the mixed organic matter field, reflecting the input of marine and terrigenous organic matter during Woodford deposition.

Sterane distributions for the Woodford Shale samples were determined through analysis of saturate and branched and cyclic fractions by GC-MS monitoring the ion at the mass-to-charge ratio (*m/z*) 217. The sterane distribution for one of the upper Woodford samples is in Figure 10, and peak identifications are presented in Table 5. In general, the C₂₉ steranes are relatively more abundant than the C₂₇ and C₂₈ steranes; however, Volkman (1986) suggested that this distribution does not necessarily indicate a higher terrigenous organic matter in-

put. The relative proportions of the C₂₇, C₂₈, and C₂₉ regular steranes were plotted on a ternary diagram (Figure 11) to determine variations resulting from organic matter source and depositional environment. According to the regular sterane ternary diagram developed by Moldowan et al. (1985), the Woodford Shale samples are clustered within the marine source rocks older than 350-Ma field, which approximately corresponds to the age and depositional environment of the source rocks analyzed. Therefore, in this case, the presence of C₂₉ steranes in the Woodford Shale samples not only represents a contribution of terrigenous organic matter to the source rocks, but also the input of marine algae.

The C₃₀ steranes (24-n-propylcholestanes) are derived from 24-n-propylcholesterols, which have been synthesized by marine algae since the Early Ordovician and the Devonian (Moldowan et al., 1990). A plot of the biomarker ratio C₃₀ steranes (20R)/C₂₉ steranes (20R) (Table 4) with depth (Figure 8) for the Wyche 1 well exhibits a very subtle change of about 118 and 185 ft (~36 and 56 m), coinciding with the upper-middle and middle-lower Woodford boundaries. These changes could indicate variations in organic matter type across the different Woodford Shale members, as

Table 3. Measured and Calculated R_o Values for Woodford Samples Used in This Study

Woodford Shale Member	Sample No.	Depth (ft)	Range of Measured R_o (%)	Calculated R_o (%)
Upper	WCWF-1*	92.21	0.53–0.72	0.63
	WCWF-2	97.92		0.62
	WCWF-3	103.00		0.60
	WCWF-4	107.08		0.49
	WCWF-5*	111.00	0.50–0.79	0.47
	WCWF-6	113.08		0.69
	WCWF-7	115.13		0.53
Middle	WCWF-8	118.04		0.45
	WCWF-9	121.17		0.53
	WCWF-10	123.13		0.47
	WCWF-11	130.41		0.31
	WCWF-12	139.15		0.49
	WCWF-13	151.08		0.38
	WCWF-14	157.83		0.42
	WCWF-15	170.45		0.26
	WCWF-16	181.04		0.36
Lower	WCWF-17	186.90		0.49
	WCWF-18	192.35		0.33
	WCWF-19	198.21		0.29
	WCWF-20*	208.08	0.55	0.42

*WCWF-1 = based on six vitrinite reflectance (R_o) measurements; WCWF-5 = based on 18 R_o measurements; WCWF-20 = based on one R_o measurement; average R_o is 0.62% based on 25 measurements; standard deviation = 0.08.

first suggested by the Pr/n-C₁₇ and Ph/n-C₁₈ ratios (Figure 9). The C₃₀ steranes (20R)/C₂₉ steranes (20R) ratio shows a decrease in the lower member and then a steady increase going upward in the sequence to the middle and upper members. This variation could account for a higher terrigenous input when the lower member was deposited and a predominance of marine organic matter input during deposition of the middle and upper members. This interpretation is consistent with the observations made by Urban (1960) in his analysis of the occurrence and distribution of microfossil assemblages within the different members of the Woodford Shale.

Hopane distributions determined by GC-MS from the m/z 191 chromatograms are shown in

Figure 12, and peak identifications are given in Table 6. The hopane/sterane ratio (Table 4) has been used to qualitatively determine prokaryote (bacteria) versus eukaryote (plankton and benthic algae) input. Hence, high hopane/sterane ratios reflect a dominant bacterial contribution generally related to terrigenous or reworked organic matter, whereas low ratios indicate major planktonic and/or benthic algae input associated with marine environments (Moldowan et al., 1985; Peters et al., 2005). The geochemical log for the Wyche 1 well (Figure 8) shows significant variations in the hopane/sterane ratio within the middle Woodford and a general decrease of these values from the lower to the upper members, suggesting a change from terrigenous to marine organic matter going upward in the sequence. This observation coincides with the C₃₀ steranes (20R)/C₂₉ steranes (20R) ratio previously described.

The distribution of the extended hopanes or homohopanes (C₃₁–C₃₅) (Figure 12) has been used to evaluate redox conditions based on the intensity of the C₃₅ homohopane compared with the C₃₄ homolog. Relatively high C₃₅ homohopane concentrations relative to C₃₄ are indicative of anoxic conditions in the water column during sediment deposition (Peters et al., 2005). With increasing depth (Figure 12), it seems that the intensity of the homohopane distribution in the Woodford Shale samples decreases relative to the tricyclic terpanes. Initially, one would think this is probably reflecting a maturity increase; however, because only 200 ft of section is being considered, this variation is unlikely to be related to thermal maturity and more likely reflects an organic facies change. The intensity of the C₃₅ homohopane remains relatively high, suggesting the existence of reducing marine conditions that allowed accumulation and preservation of the organic matter during Woodford Shale sedimentation and diagenesis.

The most abundant terpane is the C₃₀ hopane (C₃₀ 17 α [H], 21 β [H]-hopane), followed by the C₂₃ tricyclic terpane (Figure 12). The ratio C₂₃ tricyclic (cheilanthane)/C₃₀ hopane has been used to evaluate biomarkers derived from bacterial or algal sources (tricyclics) against biomarkers derived from prokaryotes (hopanes) (Peters et al., 2005). For

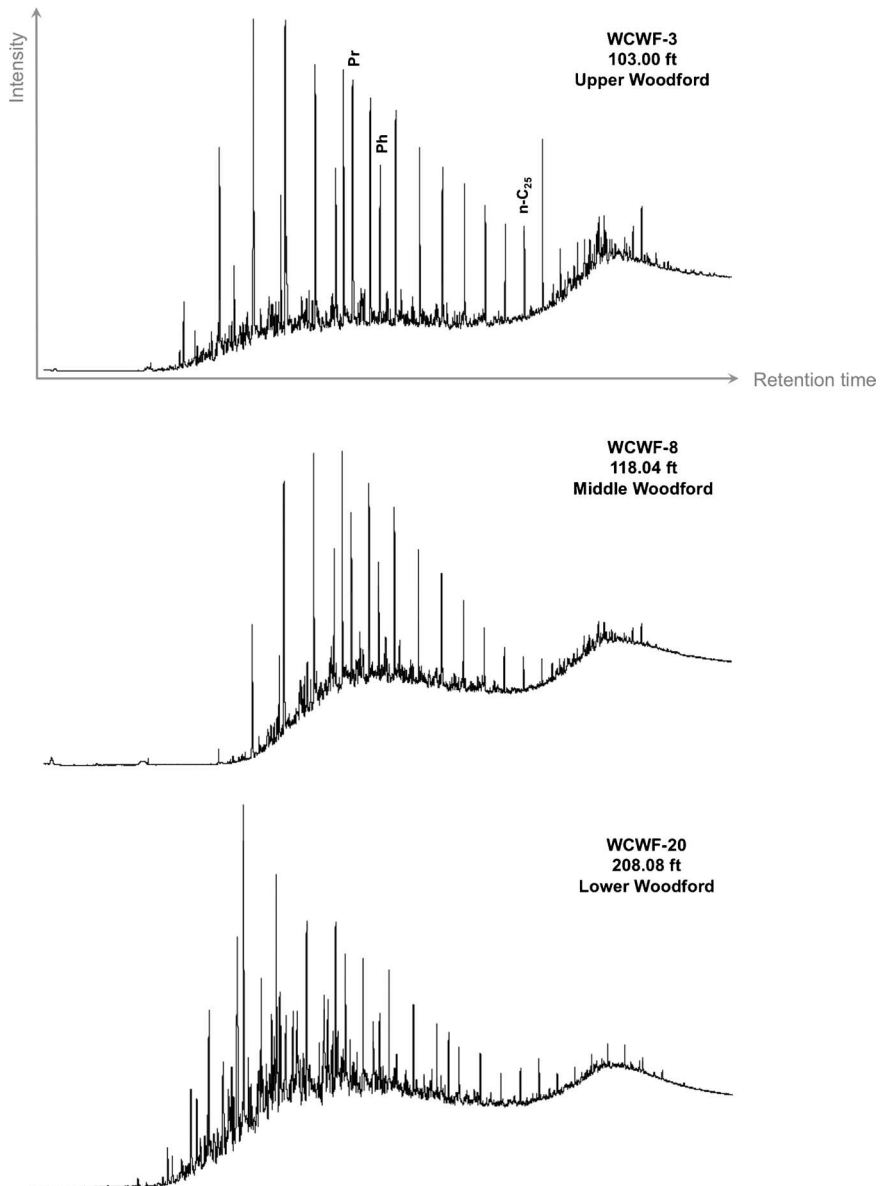


Figure 7. Gas chromatograms of saturate fractions from bitumen extracts of the Wyche 1 well. Pr = pristane; Ph = phytane; n-C₂₅ = C₂₅ normal alkane.

the Wyche 1 well (Figure 8; Table 4), the ratio increases with depth, possibly indicating a higher input of marine algae going down in the sequence. In any case, the relative abundance of the C₂₃ tricyclic terpane is another indicator that confirms the input of marine organic matter into the Woodford Shale sediments.

Gammacerane was also identified in the m/z 191 chromatograms of the Woodford Shale extracts (Figure 12). Gammacerane is a very good indicator of water column stratification during sedimentation in marine and nonmarine environments and is commonly associated with hypersaline conditions at depth (Moldowan et al., 1985; ten Haven

et al., 1989; Sinninghe Damsté et al., 1995; Peters et al., 2005). The geochemical log for the Wyche 1 well (Figure 8), featuring the gammacerane index (gammacerane/gammacerane + C₃₀ hopane), shows a higher proportion of gammacerane in the middle Woodford. This observation suggests that water stratification and salinity was an important factor in middle member deposition compared with the upper and lower members. Peters et al. (2005) indicated that a high gammacerane index resulting from water salinity and stratification correlates with a decrease in Pr/Ph ratios because of a low oxygen content in bottom waters. This relationship between gammacerane and Pr/Ph ratios is observed

Table 4. Biomarker Ratios for the Woodford Shale Samples*

Woodford Shale Member	Sample	Pr/Ph	Pr/n-C ₁₇	Ph/n-C ₁₈	Hop/Ster	C ₂₃ Tricyc/C ₃₀ Hop	Gamm Index	C ₂₉ Ster/Aryl Isoprenoids	C ₁₈ AIR	AIR
Upper	WCWF-1	2.07	1.61	0.97	0.30	0.21	0.11	1.67	6.09	2.83
	WCWF-2	1.97	1.54	0.95	0.31	0.17	0.16	2.44	6.10	3.31
	WCWF-3	1.80	1.13	0.79	0.35	0.35	0.22	0.57	12.80	2.96
	WCWF-4	1.53	0.97	0.74	0.39	0.40	0.11	0.52	12.61	2.67
	WCWF-5	1.60	1.08	0.86	0.35	0.46	0.19	0.76	12.06	2.15
	WCWF-6	1.51	0.94	0.74	0.45	0.36	0.06	0.34	10.34	2.29
	WCWF-7	1.77	0.94	0.64	0.48	0.46	0.08	0.19	7.98	2.37
Middle	WCWF-8	1.51	0.77	0.67	0.44	0.85	0.17	0.20	3.08	0.57
	WCWF-9	1.48	0.99	0.87	0.53	0.46	0.23	0.68	1.13	0.30
	WCWF-10	1.38	0.99	0.85	0.56	0.55	0.22	0.64	1.58	0.31
	WCWF-11	1.87	0.88	0.64	1.33	n.d.	n.d.	0.04	2.47	1.44
	WCWF-12	1.12	1.37	1.94	0.73	0.44	0.39	0.13	2.14	1.79
	WCWF-13	1.45	2.35	2.06	0.96	0.42	0.33	0.08	2.63	1.49
	WCWF-14	1.11	1.99	2.02	0.57	0.64	0.23	0.11	1.83	0.77
	WCWF-15	1.79	1.63	1.14	0.92	0.93	0.26	0.06	3.09	1.94
	WCWF-16	1.83	1.31	0.79	0.52	0.56	0.14	0.19	6.51	0.97
Lower	WCWF-17	1.74	1.15	0.92	0.51	0.79	0.23	0.06	6.92	2.48
	WCWF-18	2.04	1.14	0.80	0.83	0.81	n.d.	0.03	5.76	3.01
	WCWF-19	1.82	1.49	1.01	0.57	0.76	0.30	0.05	7.60	2.09
	WCWF-20	3.48	1.43	0.49	0.68	n.d.	n.d.	0.03	4.34	3.85

*Ratios were calculated based on peak heights. Pr = pristane; Ph = phytane; n-C₁₇ = C₁₇ normal alkane; n-C₁₈ = C₁₈ normal alkane; Hop = hopanes; Ster = steranes; C₂₃ tricyc = C₂₃ tricyclic terpane; Gamm Index = gammacerane index; C₂₉ ster = C₂₉ steranes; AIR = aryl isoprenoid ratio; n.d. = not determined.

for the Woodford Shale samples, which indicate higher water salinity, density stratification, and more reducing conditions during deposition of the middle Woodford unit.

Sesquiterpanes in the Woodford Shale extracts were determined by GC-MS and monitoring the ions at m/z 123 and m/z 193. Among the six bicyclic sesquiterpenoids (C₁₅) observed in the samples, eudesmane (4β[H]-eudesmane) and drimane (8β[H]-drimane) were identified. Four C₁₆ bicyclanes, including homodrimane (8β[H]-homodrimane), were also recognized (Figure 13; Table 7). Philp et al. (1981) proposed that these compounds might originate from thermal maturation of tricyclic diterpenoids, which in turn were derived from higher plant resins. However, drimane and homodrimane have been found in all types of oil and sediments, suggesting an origin from a widespread source. Structural analysis of the drimanes pointed to ho-

panoids as a potential precursor. This possibility makes it less likely that these compounds should be considered highly specific indicators of terrigenous organic matter (Alexander et al., 1984; Weston et al., 1989). However, eudesmane has been characterized as a derivative of the higher plant precursor eudesmanol; for that reason, it has been used as a biomarker for terrigenous organic matter (Philp and Gilbert, 1985; Dzou et al., 1995). Homodrimane (m/z = 123; peak 9) was widespread among all the Woodford Shale samples. On the contrary, eudesmane (m/z = 193; peak 2) was mainly present in the lower Woodford Shale, which suggests the presence of terrigenous organic matter during deposition of this member.

Aryl isoprenoids have been described as being derived from isorenieratene, a diaromatic carotenoid pigment produced by the green sulfur bacteria *Chlorobiaceae* (Brown and Kenig, 2004). Anoxic

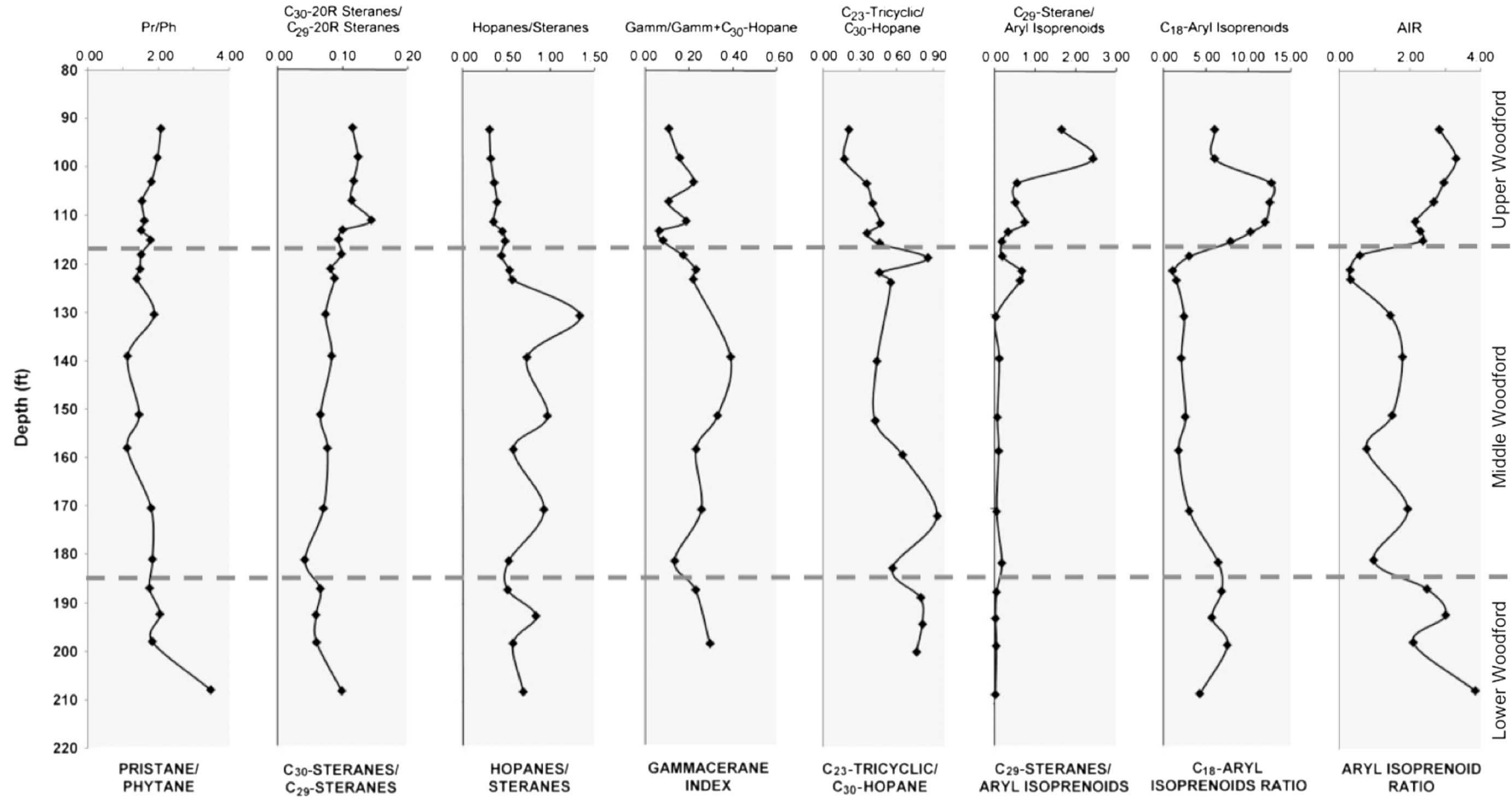
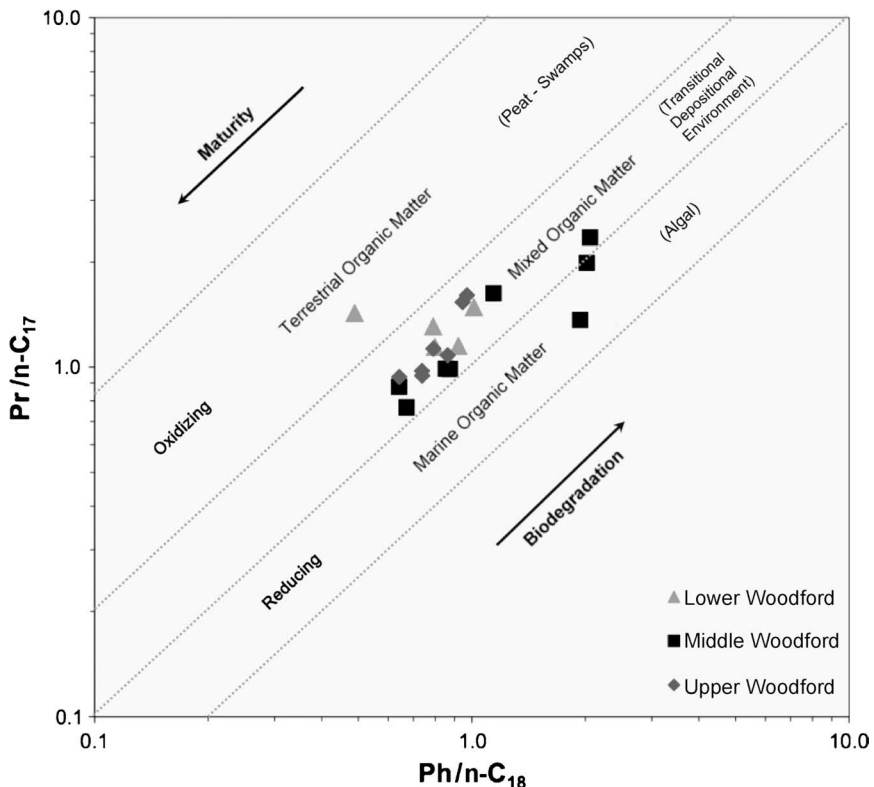


Figure 8. Geochemical logs showing different biomarker ratios for the Wyche 1 well. AIR = $(C_{13}-C_{17}/C_{18}-C_{22})$ 2,3,6-trimethyl-substituted aryl isoprenoids; C_{29} sterane/aryl isoprenoids = C_{29} sterane (20R)/2,3,6-trimethyl-substituted aryl isoprenoid; C_{18} aryl isoprenoids ratio = C_{18} 2,3,6-trimethyl-substituted aryl isoprenoid/ C_{18} 3,4,5-trimethyl-substituted aryl isoprenoid.

Figure 9. Isoprenoid plot of pristane (Pr)/n-C₁₇ versus phytane (Ph)/n-C₁₈, showing redox conditions and depositional environments for the Woodford Shale samples.



waters and the presence of H₂S and light are required for *Chlorobiaceae* to photosynthesize. Hence, aryl isoprenoids are good indicators of photic zone anoxia (PZA) and can be used as a geochemical parameter in paleoenvironmental studies.

Aryl isoprenoids were detected in the Woodford Shale samples by GC-MS of the saturate fraction and monitoring ions at m/z 133, 134. Although these compounds have an aromatic ring in their structure, they tend to elute with the saturate hydrocarbons (Brown and Kenig, 2004) because of

the presence of the long acyclic side chain substituent. The compounds identified were a series of C₁₃-C₃₁ aryl isoprenoids, but in most samples, this series extended only up to C₂₄ (Figure 14). The 1-alkyl-2,3,6-trimethylbenzenes (m/z = 133) were the most abundant in all samples, whereas the 1-alkyl-3,4,5-trimethylbenzenes (m/z = 134) were present in lower concentrations. Based on compound-specific δ¹³C analysis for different carotenoid derivatives, Koopmans et al. (1996) determined that the 2,3,6 trimethyl-substituted aryl

Figure 10. Partial fragmentograms of the m/z 217 ion showing sterane distribution in the saturate fractions of the Woodford Shale. Peak identification is presented in Table 5.

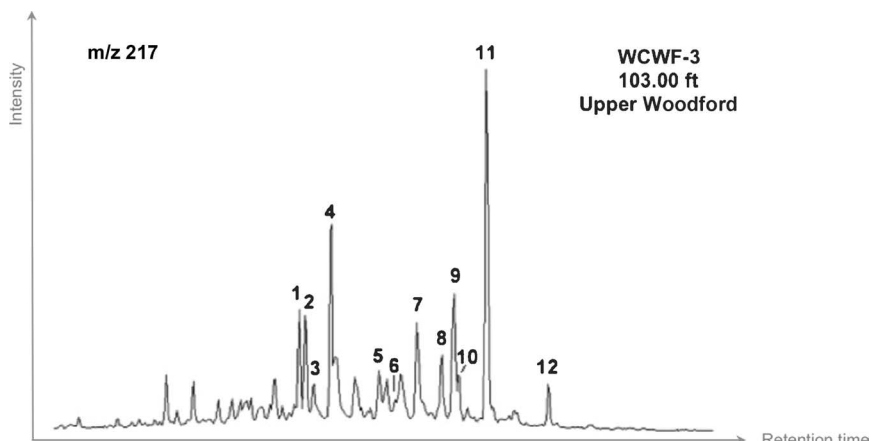


Table 5. Identification of Steranes in the Partial m/z 217 Fragmentogram

Peak No.	Compound
1	C_{28} -24-methyl-13 α (H),17 β (H)-diacholestan e (20S) + C_{27} -14 α (H),17 α (H)-cholestane (20S)
2	C_{28} -24-ethyl-13 β (H),17 α (H)-diacholestan e (20S) + C_{27} -14 β (H),17 β (H)-cholestane (20R)
3	C_{27} -14 β (H),17 β (H)-cholestane (20S) + C_{28} -24-methyl-13 α (H),17 β (H)-diacholestan e (20R)
4	C_{27} -14 α (H),17 α (H)-cholestane (20R)
5	C_{28} -24-methyl-14 α (H),17 α (H)-cholestane (20S)
6	C_{28} -24-methyl-14 β (H),17 β (H)-cholestane (20S)
7	C_{28} -24-methyl-14 α (H),17 α (H)-cholestane (20R)
8	C_{29} -24-ethyl-14 α (H)-17 α (H)-cholestane (20S)
9	C_{29} -24-ethyl-14 β (H),17 β (H)-cholestane (20R)
10	C_{29} -24-ethyl-14 β (H),17 β (H)-cholestane (20S)
11	C_{29} -24-ethyl-14 α (H),17 α (H)-cholestane (20R)
12	C_{30} -24-propyl-14 α (H),17 α (H)-cholestane (20R)

isoprenoids are also derived from β -isorenieratane and β -carotane, ruling them out as specific biomarkers for photic zone euxinia. However, similar isotopic analysis for the 3,4,5-trimethyl-substituted aryl isoprenoids indicates that they are derivatives of *Chlorobiaceae* (Brown and Kenig, 2004). As a

result, their presence in the Woodford Shale samples provides evidence of *Chlorobiaceae* and the occurrence of euxinic conditions up to the photic zone during Woodford deposition.

An interesting observation from the samples in the Wyche 1 well is an increase in the proportion of the 3,4,5-trimethyl-substituted aryl isoprenoids relative to the 2,3,6-trimethyl-substituted aryl isoprenoids in the middle member (Figure 14). The differences in concentration between the 2,3,6- and 3,4,5-trimethyl-substituted aryl isoprenoids may be a consequence of the redox conditions prevailing within the depositional environment. To verify this hypothesis, a C_{18} aryl isoprenoid ratio (AIR) was calculated, corresponding to the proportion of the C_{18} 2,3,6-trimethyl-substituted aryl isoprenoid versus the C_{18} 3,4,5-trimethyl-substituted aryl isoprenoid. The geochemical log of the C_{18} AIR for the Wyche 1 well (Figure 8) showed an abrupt decrease about 118 ft (~36), making it easy to define the upper-middle Woodford boundary. In addition, a slight increase of this ratio about 185 ft (~56 m) coincides with the middle-lower Woodford boundary. The low values of the C_{18} AIR for the samples of the middle member coincide with low Pr/Ph ratios, indicating

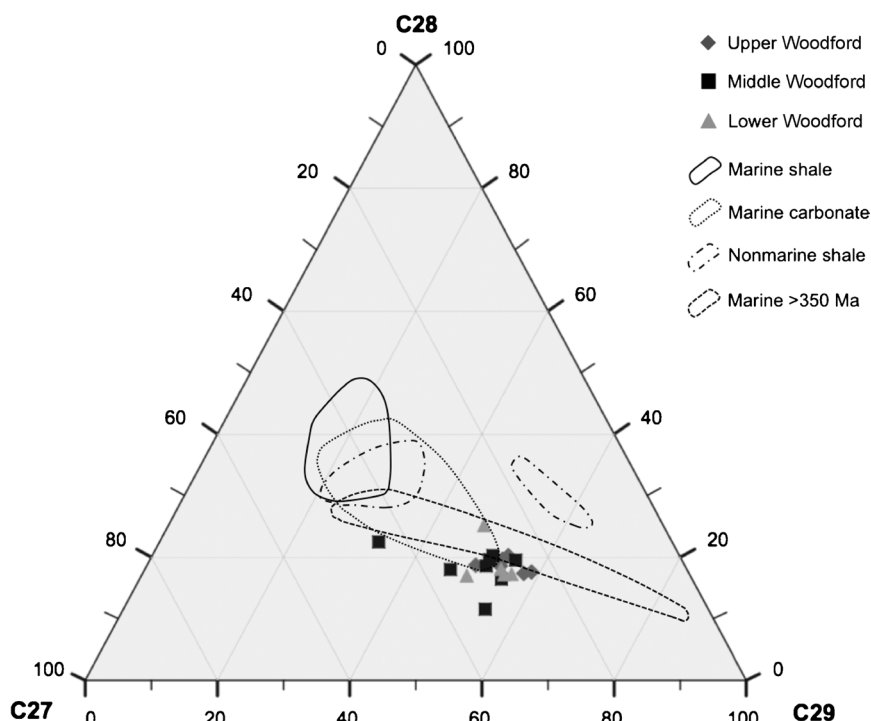
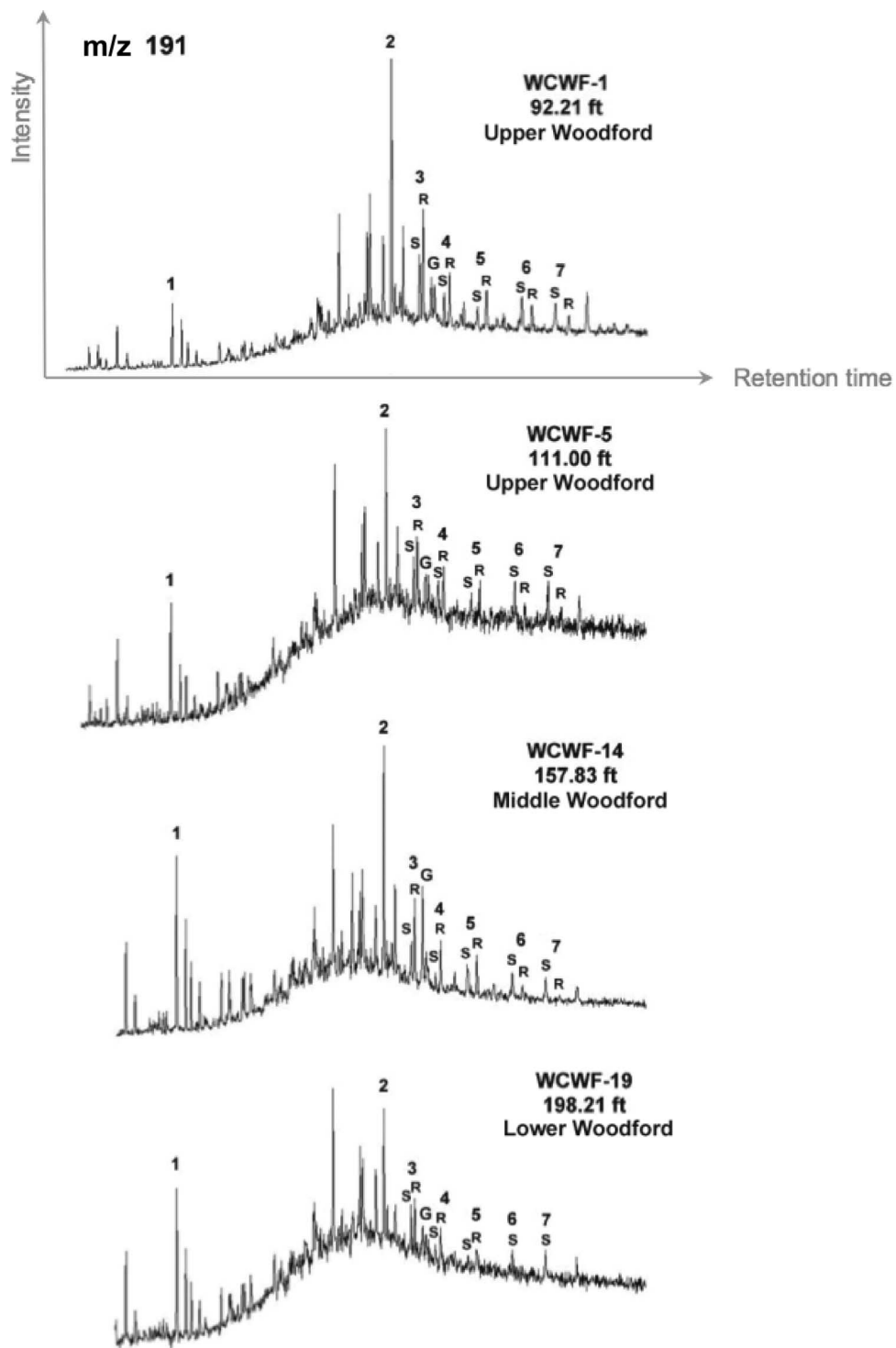


Figure 11. Ternary diagram of C_{27} , C_{28} , and C_{29} steranes for the Woodford Shale samples (plot template from Moldowan et al., 1985).

Figure 12. The m/z 191 fragmentograms showing terpane distribution in the saturate fractions of the Wyche 1 well. Peak identification is presented in Table 6.



that the presence of anoxia possibly led to the preservation of the 3,4,5-trimethyl-substituted aryl isoprenoids. In addition, from the $m/z = 133 + 134$ fragmentograms (Figure 14), it can also be observed that the intensity of the $C_{13}-C_{17}$ 2,3,6-trimethyl-substituted series is lower within the middle mem-

ber compared with the intensity of the $C_{18}-C_{22}$ 2,3,6- and the 3,4,5-trimethyl substituted aryl isoprenoids. Long-chain aryl isoprenoids are commonly altered under oxic-suboxic conditions to short-chain aryl isoprenoids. This observation suggests that anoxic conditions were a very important

Table 6. Identification of Terpanes in the m/z 191 Fragmentogram

Peak No.	Compound
1	C ₂₃ -tricyclic terpane
2	C ₃₀ -17α(H),21β(H)-hopane
3	C ₃₁ -17α(H),21β(H)-homohopanes (22S and 22R)
4	C ₃₂ -17α(H),21β(H)-bis homohopane (22S and 22R)
5	C ₃₃ -17α(H),21β(H)-tris homohopane (22S and 22R)
6	C ₃₄ -17α(H),21β(H)-tetrakis homohopane (22S and 22R)
7	C ₃₅ -17α(H),21β(H)-pentakis homohopane (22S and 22R)
G	Gammacerane

factor for preservation of long-chain aryl isoprenoids and the 3,4,5-substituted homologs during sediment deposition and diagenesis of the middle Woodford.

The C₂₉ sterane/AIR was calculated from the C₂₉ steranes (20R) and the aryl isoprenoid peaks using the summed mass chromatograms of the m/z 217 + 218 and m/z 133 + 134 ions, respectively (Figure 15), and lower values indicate a higher proportion of aryl isoprenoids in the samples. On the geochemical log for this ratio, it can be observed that a significant change in the distribution of these compounds exists in the upper-middle Woodford boundary (Figure 8). This variation may indicate a

change in redox conditions from anoxic H₂S waters during middle Woodford deposition to dysoxic to suboxic conditions during deposition of the upper member. A small increase of this ratio about 185 ft (~56 m) suggests dysoxic to anoxic conditions for the lower member.

Because aryl isoprenoids are indicative of the existence of PZA during sediment deposition, a more specific evaluation of the distribution of the 2,3,6-trimethyl substituted aryl isoprenoids was undertaken. The AIR was defined by Schwark and Frimmel (2004) to assess the variability and extent of PZA by calculating the proportions of the short-chain (C₁₃-C₁₇) against the intermediate-chain (C₁₈-C₂₂) 2,3,6-trimethyl substituted aryl isoprenoids. According to these authors, episodic PZA leads to alteration of the long-chain, high molecular weight aryl isoprenoids resulting in high AIR values (3.0). Conversely, persistent periods of PZA allow preservation of the long-chain aryl isoprenoids resulting in a low AIR (0.5). A depth profile of this ratio for the Wyche 1 well (Figure 8) shows a sharp decrease about 118 ft (~36). The AIR fluctuates within the middle member until an increase in the AIR at about 185 ft (~56 m) marks the boundary of the middle-lower member, indicating episodic PZA similar to the upper Woodford member. The AIR variations within the middle member correlate with higher gammacerane ratios

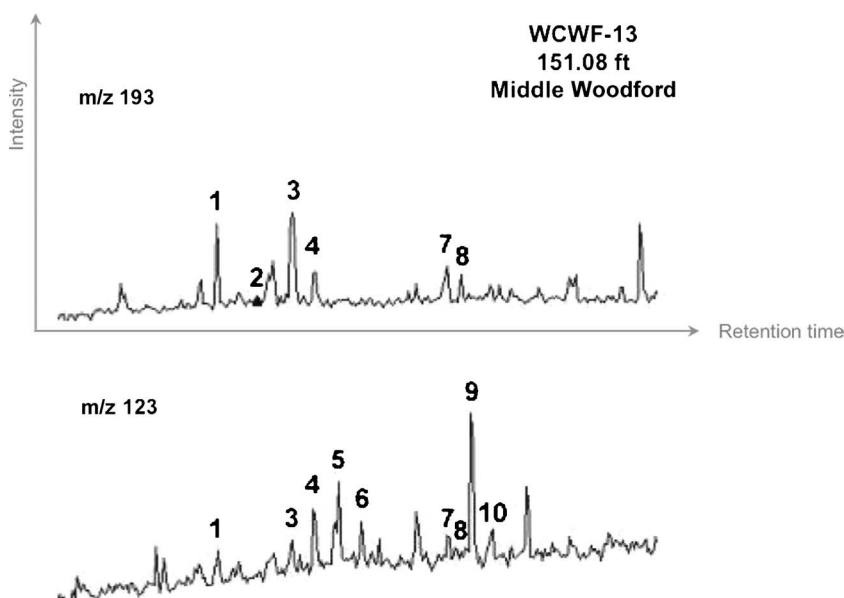


Figure 13. Partial m/z 123 and 193 chromatograms showing the bicyclic alkane distributions from the saturate fractions of the Woodford Shale samples. Peak identification is presented in Table 7.

Table 7. Identification of Bicyclic Alkanes in the m/z 193 and 123 Chromatograms

Peak No.	Compound
1	C ₁₅ -sesquiterpane
2	C ₁₅ -4β(H)-eudesmane
3	C ₁₅ -sesquiterpane
4	C ₁₅ -8β(H)-drimane
5	C ₁₅ -sesquiterpane
6	C ₁₅ -8α(H)-drimane
7	C ₁₆ -sesquiterpane
8	C ₁₆ -sesquiterpane
9	C ₁₆ -8β(H)-homodrimane
10	C ₁₆ -sesquiterpane

and lower Pr/Ph ratios, supporting the relationship between water stratification, hypersalinity, redox conditions, and aryl isoprenoid distributions.

To better define this relationship for the Woodford Shale samples, a plot of AIR versus Pr/Ph was constructed according to the guidelines proposed by Schwark and Frimmel (2004) (Figure 16). In this diagram, two different groups can be observed. Within group 1, samples of the upper and lower Woodford appear to have experienced similar redox conditions. The cluster encompassing these samples exhibits high AIR and relatively high Pr/Ph values, indicating the occurrence of episodic PZA. On the contrary, group 2, which is dominated by samples from the middle member, appears to have been influenced by more persistent euxinic conditions during deposition.

Paleoenvironmental Interpretation

The presence of *Chlorobiaceae* derivatives along the Woodford Shale profile is indicative of PZA. Variations in the AIR indicate episodic PZA for the upper and lower members and more persistent PZA conditions in the middle member. According to Schwark and Frimmel (2004), the variations in concentration of the aryl isoprenoids in sediments reflect *Chlorobiaceae* productivity. Therefore, they reflect how much anoxia extended into the photic zone and the stability of water column stratification. Moreover, this information gives indication about fluctuations of the chemocline, as suggested

by Sinnighe Damsté et al. (1993) and Brown and Kenig (2004).

Variations related to depositional environments and type of organic matter within the different Woodford Shale members are summarized with the biomarker ratios presented in Figure 8. Ratios of the C₃₀ steranes/C₂₉ steranes, hopanes/steranes, C₂₃ tricyclic/C₃₀ hopanes indicate that the Woodford Shale members are characterized by a mix of terrigenous and marine organic matter, whereas the middle member shows the greatest marine input. Based on Pr/Ph and AIRs, the lower and upper members are characterized by dysoxic to suboxic conditions. In contrast, the middle Woodford shows a predominance of euxinic and/or anoxic conditions. The presence of gammacerane, a biomarker typically associated with hypersaline conditions (Sinninghe Damsté et al., 1995; Peters et al., 2005), indicates that high water salinity and water density stratification prevailed during most of Woodford Shale deposition, especially for the middle member, which shows higher gammacerane index values. These observations suggest that deposition of the middle member was characterized by higher organic productivity and preservation, where the chemocline was located at shallower depths into the photic zone. On the contrary, during deposition of the lower and upper members, sea level fluctuations produced an intermittent depth change of the chemocline, resulting in episodic euxinia, where oxidative periods degraded part of the organic matter.

Paxton et al. (2007) were able to define regressive and transgressive cycles within the Woodford Shale based on gamma-ray readings. Buckner et al. (2009) and Slatt et al. (2011) also established these cycles from the gamma-ray log of the Wyche 1 well in a similar way as Paxton et al. (2007). Here, an attempt has been made to establish sea level changes during Woodford deposition based on a geochemical parameter called relative hydrocarbon potential (RHP). These observations are also correlated with the regressive-transgressive cycles and the sequence-stratigraphic framework of the Woodford Shale defined by Buckner et al. (2009) and Slatt et al. (2011).

The RHP is a geochemical parameter derived from Rock-Eval pyrolysis data ([S₁ + S₂]/TOC) to

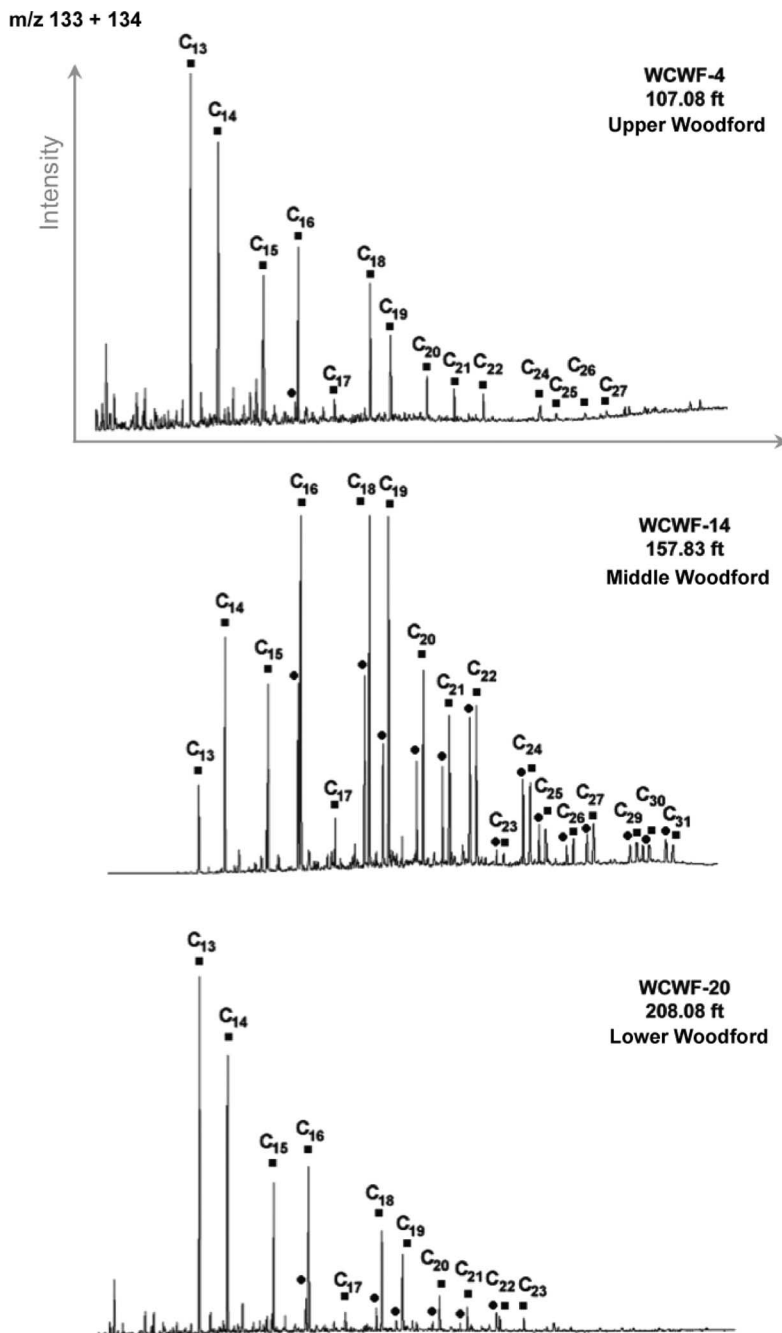
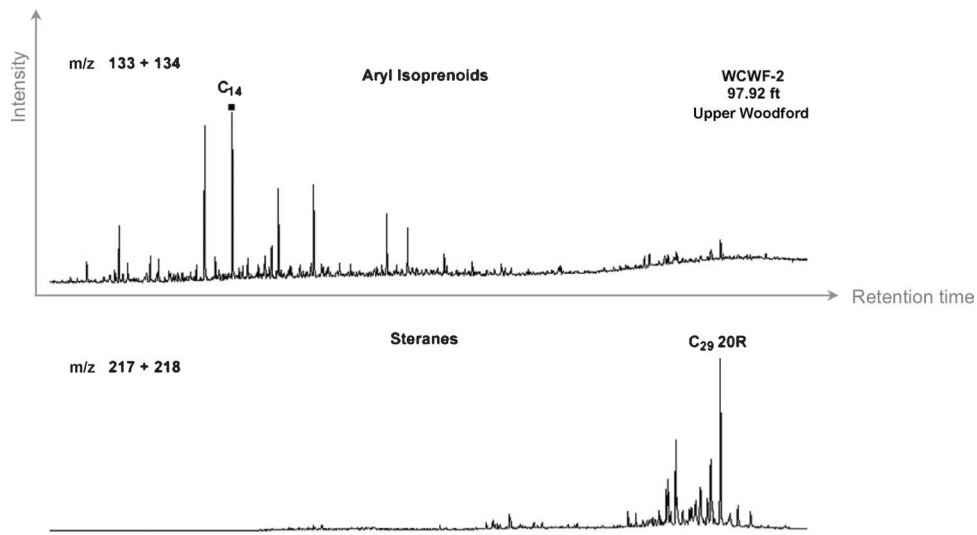


Figure 14. Summed mass chromatograms of m/z 133, 134 of the saturate fractions showing the aryl isoprenoid distribution for the Wyche 1 well samples. Filled squares = 2,3,6-trimethyl-substituted aryl isoprenoids; filled circles = 3,4,5-trimethyl substituted aryl isoprenoids. The number of carbon atoms is indicated above each peak.

characterize depositional environments and their temporal variations (Fang et al., 1993; Singh, 2008; Slatt et al., 2009d). Fang et al. (1993) were the first to use this parameter to define vertical organic facies changes called vertical organic facies sequence (VOFS). Based on RHP, they established two main VOFSs, rising-upward and falling-upward sequences. The rising-upward VOFS represents a vertical change in organic facies from hydrogen poor to hydrogen rich going up the stratigraphic

sequence; it indicates a change from oxic to anoxic conditions (sea level rise), where most of the organic matter is preserved. On the contrary, the falling-upward VOFS represents a vertical change in organic facies from hydrogen rich to hydrogen poor, thus, this VOFS indicates a change from anoxic to oxic conditions (sea level fall), where less organic matter is preserved. From this, definitions of regressive-transgressive cycles can be applied to sequence stratigraphy.

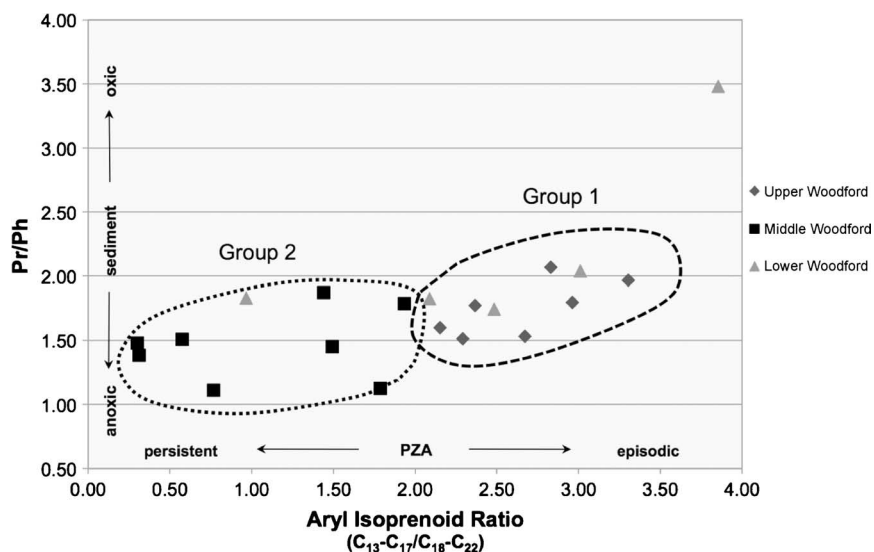
Figure 15. Summed mass fragmentograms of ions m/z 133, 134 and m/z 217, 218, showing the aryl isoprenoid and sterane distribution for calculation of the C₂₉ steranes/aryl isoprenoids ratio. Filled square = 2,3,6-trimethyl-substituted aryl isoprenoid.



The RHP analysis in the Wyche 1 well revealed five falling and five rising stages of sea level in the Woodford Shale (Figure 17). These variations in the RHP curve indicate several cycles of transgression and regression that positively correlate with the transgressive-regressive cycles and sequence stratigraphy defined by Buckner et al. (2009) and Slatt et al. (2011). The base of the lower Woodford is characterized by a major transgression followed by a small regression, which ended with another transgression and the development of a possible transgressive surface of erosion at the lower-middle Woodford boundary. According to the sequence-stratigraphic framework proposed by Slatt et al. (2011), this interval appears to correspond to a

transgressive/highstand systems tract (TST/HST) and represents dysoxic to suboxic conditions, as indicated by Pr/Ph ratios and biomarkers. In the case of the middle Woodford, a major transgression is observed related to a possible TST (sea level rise). The Pr/Ph ratios indicate variations in redox conditions; however, the low values suggest that anoxic conditions prevailed during deposition of this member. Krystyniak (2003) reported that the middle member of the Woodford Shale contains higher amounts of uranium compared with the other members. Because it is a redox-sensitive element, uranium is a good indicator for paleoredox conditions and organic productivity. Under reducing conditions, uranium is insoluble and is removed

Figure 16. Pristane (Pr)/phytane (Ph) versus aryl isoprenoid ratio (AIR) plot for the Woodford Shale samples showing two distinctive groups based on variations and degree of photic zone anoxia (PZA) (plot template from Schwark and Frimmel, 2004).



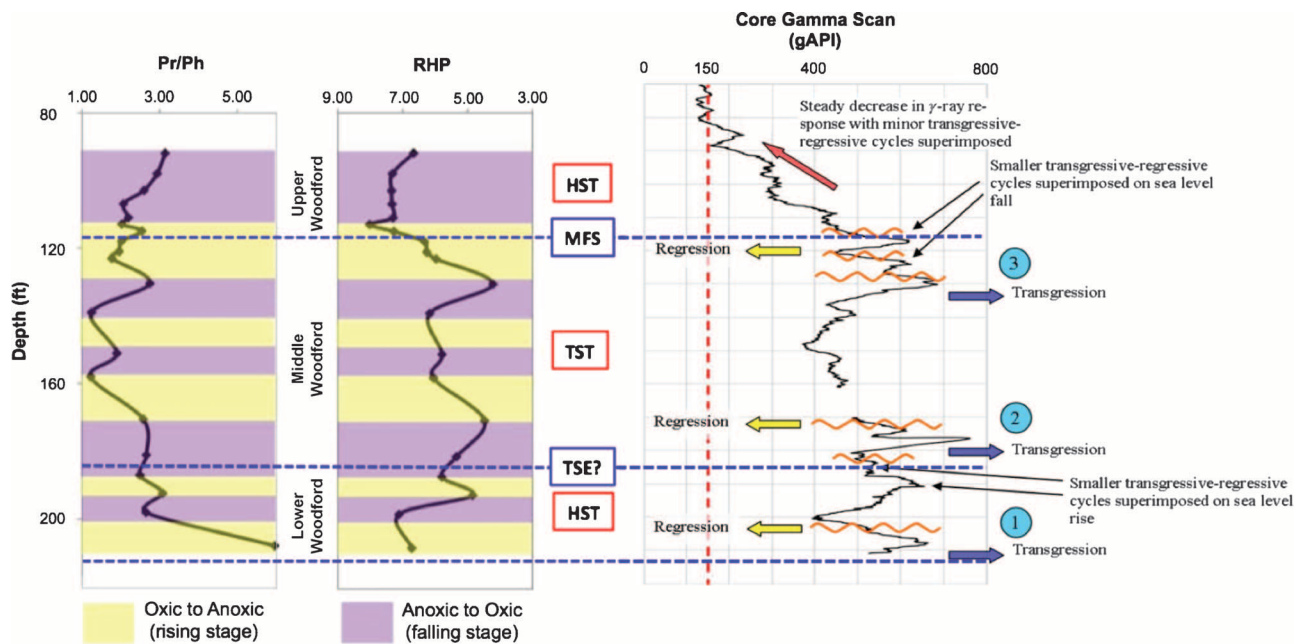


Figure 17. Pristane (Pr)/phytane (Ph) ratio, relative hydrocarbon potential (RHP), and core gamma scan for the Wyche 1 well showing variations in redox conditions and regressive-transgressive cycles linked to the sequence stratigraphy of the Woodford Shale. HST = highstand systems tract; MFS = maximum flooding surface; TST = transgressive systems tract; TSE = transgressive surface of erosion. Squiggles represent unconformities. Core gamma scan and sequence-stratigraphic interpretations are from Slatt et al. (2011).

from sea water and incorporated into organic-rich hemipelagic sediments (Klinkhammer and Palmer, 1991). Therefore, the elevated amounts of uranium in the middle Woodford Shale indicate an anoxic environment during its deposition. According to Slatt et al. (2011), the middle-upper Woodford boundary corresponds to a maximum flooding surface and is followed by a general regression, which indicates that deposition of the upper member occurred during a highstand with a high sediment input. Hence, we expected to find that the redox conditions were dysoxic to suboxic during sediment deposition of the upper member, which is exactly what the Pr/Ph ratios and biomarkers showed in this interval.

Woodford Shale deposition was influenced by sea level changes, which in turn affected redox conditions and the extent of anoxia. These variations had a direct effect in the type and amount of organic matter that accumulated and was preserved within the sediments and determined the organic richness of the Woodford Shale in this area. A method that could significantly contribute to complete and further understand these interpretations

is to apply this study on a regional context and to integrate and correlate these data with a sequence-stratigraphic framework, an approach that has succeeded in other shale gas plays (Singh, 2008; Slatt et al., 2009d).

CONCLUSIONS

In southeastern Oklahoma, the Woodford Shale is organic rich, with TOC values ranging from 5.01 to 14.81%. These values indicate that this formation is an excellent potential source rock for hydrocarbon generation. According to Rock-Eval data, the Woodford Shale is dominated by type II kerogen, containing oil- and gas-prone marine organic matter. Variations in the high HI values for these samples can be attributed to organic facies variations along the analyzed section.

The Woodford Shale in southeastern Oklahoma is immature, as expressed by measured and calculated R_o values and Rock-Eval data. Because of its low maturity and based on observations from similar shale gas plays, it is unlikely that the Woodford

Shale has generated large quantities of hydrocarbons in this area.

Biomarker analyses reveal variations in redox conditions and a mix of organic matter input. A comparison of the generated geochemical logs and available geologic data permitted dividing the Woodford Formation into upper, middle, and lower members. A mix of terrigenous and marine organic matter characterizes the three Woodford Shale members, with the middle member showing the greatest marine input.

Integration and correlation of Pr/Ph ratios, AIRs, and RHP indicate that the lower Woodford was deposited under dysoxic to suboxic conditions and episodic periods of PZA during a major transgressive-regressive-transgressive cycle; the middle Woodford was deposited under anoxic conditions and persistent PZA during a major transgression (sea level rise); and the upper Woodford was deposited under dysoxic to suboxic conditions and episodic PZA during a general regression (HST with high sedimentation rate). These interpretations are consistent with a sequence-stratigraphic framework already proposed for the Woodford Shale in the study area.

High-salinity conditions and water density stratification also prevailed during deposition of the Woodford Shale. The chemocline was located at shallower depths during middle Woodford deposition and fluctuated within different depths during deposition of lower and upper members.

The RHP ratio constitutes a valuable parameter for evaluating sea level changes that can be linked to regressive-transgressive cycles and consequently to temporal variations in depositional environments. Correlation of this parameter to biomarker analysis and geologic data can be effective in establishing sequence-stratigraphic frameworks, especially in shale gas plays.

APPENDIX: EXPERIMENTAL METHODS

Preliminary Sample Treatment

All the samples were washed with hot water, distilled water, and a 1:1 mixture of dichloromethane (CH_2Cl_2) and methanol (CH_3OH) to remove any contaminants (e.g., drilling mud,

plastic wrap, and handling). After the samples were completely air-dried, they were crushed with a porcelain mortar and pestle until fine powder was obtained for screening analysis (TOC and Rock Eval) and Soxhlet extraction.

Total Organic Carbon and Rock-Eval Pyrolysis

Twenty crushed rock samples were sent to Humble Geochemical Services for TOC determination and Rock-Eval pyrolysis. Approximately 1 g of each sample was needed to perform these analyses.

Vitrinite Reflectance

Measured vitrinite reflectance (R_o) values from the Wyche 1 well were obtained from pellets (whole-rock method) prepared at the Oklahoma Geological Survey Organic Petrography Laboratories in Norman, Oklahoma, and measured at the University of Oklahoma Organic Geochemistry Laboratories by Tsigabu Gebrehiwet. Calculated R_o values were provided by Humble Geochemical Services. These values are obtained from Rocaval T_{\max} data according to the equation proposed by Jarvie et al. (2001):

$$\text{Calculated \%VR}_o = 0.0180 \times T_{\max} - 7.16 \quad (1)$$

Extraction and Fractionation

A Soxhlet extraction device was preextracted for 24 hr using a 1:1 mixture of dichloromethane (CH_2Cl_2) and methanol (CH_3OH) to remove contaminants. Samples (50 g) were extracted with the same solvent mixture for 24 hr. The excess solvent from the bitumen extract was evaporated using a rotary evaporator, and the residues were transferred to a glass centrifuge tube for asphaltene precipitation. The extract was separated into maltenes and asphaltenes by adding an excess of n-pentane (C_5H_{12}). The centrifuge tubes were placed in a freezer overnight to promote complete asphaltene precipitation.

The maltenes fractions were transferred to 250-mL round-bottom flasks to evaporate the solvent excess and then placed in vials. This fraction was then diluted in a ratio of 2-mg sample/50 μL hexane (C_6) for fractionation into saturates; aromatics; and nitrogen, sulfur, oxygen compounds (resins) by high-performance liquid chromatography in a Hewlett Packard 1050 series HPLC. The saturate and aromatic fractions were diluted using 1 mL of dichloromethane per 3 mg of sample.

The n-alkanes were removed from the saturate fraction through molecular sieving. A Pasteur pipette was packed with approximately 2 g of HI-SIV 3000, and three bed volumes of C_6 were added to remove impurities. The sample was added to the column, and it was allowed to stand for 2 min. Then three additional bed volumes of C_6 were used to elute the sample. The n-alkanes were retained in the sieve whereas the

branched and cyclic compounds eluted from the column. This fraction was also diluted with 1 mL of dichloromethane/3 mg of sample.

Gas Chromatography

The instrument used for GC analyses was an Agilent 6890 series gas chromatograph with a split-splitless capillary injection system equipped with a 100 m × 0.25 mm (internal diameter) J&D Scientific DB-1 Petro 122-10A6 fused silica capillary column coated with a 0.5-μm liquid film. The temperature program for analyses started with an initial temperature of 40°C, with 1.5 min hold time. The temperature was increased to 310°C at a rate of 4°C/min followed by an isothermal period of 31 min for a total run of 100 min. The injector and flame ionization detector temperatures were set at 300 and 310°C, respectively. Samples were analyzed in splitless mode injection using helium as the carrier gas and a flow rate of 0.5 mL/min.

Gas Chromatography–Mass Spectrometry

The GCMS analyses were conducted with a Varian 3400 GC inlet system coupled to a Finnigan MAT 70 triple-stage quadrupole mass spectrometer. For biomarker analysis, selected ions were chosen to analyze samples in single ion monitoring or multiple ion detection mode. The mass spectrometer operated with one quadrupole in the single-stage mode.

The ion source operated in an electron impact mode with energy of 70 eV. The GC used a 60 m × 0.32 mm (internal diameter) J&D Scientific DB-5 fused silica capillary column coated with a 0.25-μm liquid film. The temperature program for the analyses started at 40°C, with 1.5 min hold time and was later increased to 310°C at a rate of 4°C/min and then held isothermal for 31 min. The ion source temperature was 200°C, the injector temperature was 300°C, and the transfer line temperature was 310°C.

REFERENCES CITED

- Alexander, R., R. I. Kagi, R. Noble, and J. K. Volkman, 1984, Identification of some bicyclic alkanes in petroleum: *Organic Geochemistry*, v. 6, p. 63–70, doi:[10.1016/0146-6380\(84\)90027-5](https://doi.org/10.1016/0146-6380(84)90027-5).
- Boyer, C., J. Kieschnik, R. Suarez-Rivera, R. E. Lewis, and G. Waters, 2006, Producing gas from its source: Schlumberger Oilfield Review, Autumn 2006, p. 36–49.
- Brown, T. C., and F. Kenig, 2004, Water column structure during deposition of Middle Devonian–Lower Mississippian black and green/gray shales of the Illinois and Michigan basins: A biomarker approach: *Palaeogeography, Palaeoclimatology, Palaeoecology*, v. 215, p. 59–85.
- Buckner, T. N., R. M. Slatt, B. Coffey, and R. J. Davis, 2009, Stratigraphy of the Woodford Shale from behind-outcrop drilling, logging, and coring: AAPG Search and Discovery article 50147: http://www.searchanddiscovery.com/documents/2009/50147buckner/ndx_buckner.pdf (accessed September 21, 2009).
- Burruss, R. C., and J. R. Hatch, 1989, Geochemistry of oils and hydrocarbon source rocks, Greater Anadarko Basin: Evidence for multiple sources of oils and long-distance oil migration, in K. S. Johnson, ed., Anadarko Basin: 1988 Symposium Oklahoma Geological Survey Circular 90, p. 53–64.
- Cardott, B. J., 2005, Overview of unconventional energy resources of Oklahoma, in B. J. Cardott, ed., Unconventional energy resources in the southern mid-continent: 2004 Symposium Oklahoma Geological Survey Circular 110, p. 7–18.
- Comer, J. B., 2007, Lithologic characteristics and gas production potential of Woodford Shale in the southern mid-continent (abs.): Geological Society of America Annual Meeting and Exposition, Abstracts with Programs, p. 356.
- Comer, J. B., 2008, Reservoir characteristics and production potential of the Woodford Shale: World Oil Magazine, v. 229, <http://petesplace-peter.blogspot.com/2008/08/woodford-shale-major-new-unconventional.html> (accessed October 4, 2009).
- Comer, J. B., 2009, The forms of quartz and dolomite in Woodford Shale of the southern mid-continent, U.S.A.: Indicators of paleoclimate, paleogeography, paleoceanography, and depositional processes (abs.): AAPG Mid-Continent Meeting, Book of Abstracts, p. 21.
- Curtis, J. B., 2002, Fractured shale-gas systems: AAPG Bulletin, v. 86, no. 11, p. 1921–1938, doi:[10.1306/61EEDDBE-173E-11D7-8645000102C1865D](https://doi.org/10.1306/61EEDDBE-173E-11D7-8645000102C1865D).
- Dzou, L. I. P., R. A. Noble, and J. T. Senftle, 1995, Maturation effects on absolute biomarker concentration in a suite of coals and associated vitrinite concentrates: *Organic Geochemistry*, v. 237, p. 681–697, doi:[10.1016/0146-6380\(95\)00035-D](https://doi.org/10.1016/0146-6380(95)00035-D).
- Ellison Jr., S. P., 1950, Subsurface Woodford Black Shale, west Texas and southeast New Mexico: Austin, Texas, University of Texas, Bureau of Economic Geology Report of Investigations 7, p. 5–21.
- Fang, H., C. Jianyu, S. Yongchuan, and L. Yaozong, 1993, Application of organic facies studies to sedimentary basin analysis: A case study from the Yitong graben, China: *Organic Geochemistry*, v. 201, p. 27–42, doi:[10.1016/0146-6380\(93\)90078-P](https://doi.org/10.1016/0146-6380(93)90078-P).
- Fritz, R. D., and E. A. Beaumont, 2001, Depositional environment and sequence stratigraphy of Silurian through Mississippian strata in the mid-continent, in K. S. Johnson, ed., Silurian, Devonian, and Mississippian geology and petroleum in the southern mid-continent: 1999 Symposium Oklahoma Geological Survey Circular 105, p. 173.
- Gale, J. F. W., R. M. Reed, and J. Holder, 2007, Natural fractures in the Barnett Shale and their importance for hydraulic fracture treatments: AAPG Bulletin, v. 91, no. 4, p. 603–622, doi:[10.1306/11010606061](https://doi.org/10.1306/11010606061).
- Ham, W. E., 1973, Regional geology of the Arbuckle Mountains, Oklahoma: Oklahoma Geological Survey, Guidebook for Field Trip 5, p. 1–17.

- Hester, T. C., J. W. Schmoker, and H. L. Sahl, 1990, Log-derived regional source rock characteristics of the Woodford Shale, Anadarko Basin, Oklahoma: U.S. Geological Survey Bulletin, v. 1866-D, p. 1–38.
- Hickey, J. J., and B. Henk, 2007, Lithofacies summary of the Mississippian Barnett Shale, Mitchell 2 T. P. Sims well, Wise County, Texas: AAPG Bulletin, v. 91, no. 4, p. 437–443, doi:[10.1306/12040606053](https://doi.org/10.1306/12040606053).
- Hill, R. J., D. M. Jarvie, J. Zumberge, M. Henry, and R. M. Pollastro, 2007a, Oil and gas geochemistry and petroleum systems of the Fort Worth Basin: AAPG Bulletin, v. 91, no. 4, p. 445–473, doi:[10.1306/11030606014](https://doi.org/10.1306/11030606014).
- Hill, R. J., E. Zhang, B. J. Katz, and T. Yongchun, 2007b, Modeling of gas generation from the Barnett Shale, Fort Worth Basin, Texas: AAPG Bulletin, v. 91, no. 4, p. 501–521, doi:[10.1306/12060606063](https://doi.org/10.1306/12060606063).
- Hunt, J. M., 1995, Petroleum geochemistry and geology: New York, W. H. Freeman and Company, 743 p.
- Jarvie, D. M., B. L. Claxton, F. Henk, and J. T. Breyer, 2001, Oil and shale gas from the Barnett Shale, Fort Worth Basin, Texas (abs.): AAPG Annual Meeting Abstracts, p. A100.
- Jarvie, D. M., R. J. Hill, and R. M. Pollastro, 2005, Assessment of the gas potential and yields from shales: The Barnett Shale model: Oklahoma Geological Survey Circular 110, p. 37–50.
- Jarvie, D. M., R. J. Hill, T. E. Ruble, and R. M. Pollastro, 2007, Unconventional shale-gas systems: The Mississippian Barnett Shale of north-central Texas as one model for thermogenic shale-gas assessment: AAPG Bulletin, v. 91, no. 4, p. 475–499, doi:[10.1306/12190606068](https://doi.org/10.1306/12190606068).
- Jones, P. J., and R. P. Philp, 1990, Oils and source rocks from Pauls Valley, Anadarko Basin, Oklahoma, U.S.A.: Applied Geochemistry, v. 5, p. 429–448, doi:[10.1016/0883-2927\(90\)90019-2](https://doi.org/10.1016/0883-2927(90)90019-2).
- Kinley, T. J., L. W. Cook, J. A. Breyer, D. M. Jarvie, and A. B. Busbey, 2008, Hydrocarbon potential of the Barnett Shale Mississippian, Delaware Basin, west Texas and southeastern New Mexico: AAPG Bulletin, v. 92, no. 8, p. 967–991, doi:[10.1306/03240807121](https://doi.org/10.1306/03240807121).
- Kirkland, D. W., R. E. Denison, D. M. Summers, and J. R. Gormly, 1992, Geology and organic geochemistry of the Woodford Shale in the Criner Hills and western Arbuckle Mountains, Oklahoma, in K. S. Johnson and B. J. Cardott, eds., Source rocks in the southern mid-continent: 1990 Symposium Oklahoma Geological Survey Circular 93, p. 38–69.
- Klinkhammer, G. P., and M. R. Palmer, 1991, Uranium in the oceans: Where it goes and why: Geochimica et Cosmochimica Acta, v. 55, p. 1799–1806, doi:[10.1016/0016-7037\(91\)90024-Y](https://doi.org/10.1016/0016-7037(91)90024-Y).
- Koopmans, M. P., S. Schouten, M. E. L. Kohnen, and J. S. Sinninghe Damsté, 1996, Restricted utility of aryl isoprenoids as indicators for photic zone anoxia: Geochimica et Cosmochimica Acta, v. 60, no. 23, p. 4873–4876, doi:[10.1016/S0016-7037\(96\)00303-1](https://doi.org/10.1016/S0016-7037(96)00303-1).
- Krystyniak, A. M., 2003, Outcrop-based gamma ray characterization of the Woodford Shale of south-central Oklahoma: M.S. thesis, Oklahoma State University, Stillwater, Oklahoma, 131 p.
- Lambert, M. W., 1993, Internal stratigraphy and organic facies of the Devonian–Mississippian Chatanooga Woodford Shale in Oklahoma and Kansas, in B. J. Katz and L. M. Pratt, eds., Source rocks in a sequence-stratigraphic framework: AAPG Studies in Geology 37, p. 163–176.
- Loucks, R. G., and S. C. Ruppel, 2007, Mississippian Barnett Shale: Lithofacies and depositional setting of a deep-water shale-gas succession in the Fort Worth Basin, Texas: AAPG Bulletin, v. 91, no. 4, p. 579–601, doi:[10.1306/11020606059](https://doi.org/10.1306/11020606059).
- Moldowan, J. M., W. K. Seifert, and E. J. Gallegos, 1985, Relationship between petroleum composition and depositional environment of petroleum source rocks: AAPG Bulletin, v. 69, no. 8, p. 1255–1268.
- Moldowan, J. M., F. J. Fago, C. Y. Lee, S. R. Jacobson, N. Slougui, A. Jegannathan, and D. C. Young, 1990, Sedimentary 24-n-propylcholestanes, molecular fossils diagnostic of marine algae: Science, v. 247, p. 309–312, doi:[10.1126/science.247.4940.309](https://doi.org/10.1126/science.247.4940.309).
- Northcutt, R. A., K. S. Johnson, and G. C. Hinshaw, 2001, Geology and petroleum reservoirs in Silurian, Devonian, and Mississippian rocks in Oklahoma, in K. S. Johnson, ed., Silurian, Devonian, and Mississippian geology and petroleum in the southern mid-continent: 1999 Symposium Oklahoma Geological Survey Circular 105, p. 1–29.
- Paxton, S. T., A. Cruse, and A. Krystyniak, 2007, Fingerprints of global sea level change revealed in hydrocarbon source rock?: <http://www.searchanddiscovery.net/documents/2006/06095paxton/images/paxton.pdf> (accessed September 18, 2009).
- Peters, K. E., 1986, Guidelines for evaluating petroleum source rock using programmed pyrolysis: AAPG Bulletin, v. 70, no. 3, p. 318–329.
- Peters, K. E., and M. R. Cassa, 1994, Applied source rock geochemistry, in L. B. Magoon and W. G. Dow, eds., The petroleum system: From source to trap: AAPG Memoir 60, p. 93–120.
- Peters, K. E., C. C. Walters, and J. M. Moldowan, 2005, The biomarker guide: Biomarkers and isotopes in petroleum exploration and earth history: New York, Cambridge University Press, v. 2, 1155 p.
- Philp, R. P., 2007, The role of geochemistry in characterization of gas shales and produced gas (abs.): Geological Society of America Annual Meeting and Exposition, Abstracts with Programs, p. 356.
- Philp, R. P., and T. D. Gilbert, 1985, Biomarker distribution in Australian oils predominantly derived from terrigenous source material: Organic Geochemistry, v. 10, p. 73–84, doi:[10.1016/0146-6380\(86\)90010-0](https://doi.org/10.1016/0146-6380(86)90010-0).
- Philp, R. P., T. D. Gilbert, and J. Friedrich, 1981, Bicyclic sesquiterpenoids and diterpenoids in Australian crude oils: Geochimica et Cosmochimica Acta, v. 45, p. 1173–1180, doi:[10.1016/0016-7037\(81\)90140-X](https://doi.org/10.1016/0016-7037(81)90140-X).
- Philp, R. P., P. J. Jones, L. H. Lin, G. E. Michael, and C. A. Lewis, 1989, An organic geochemical study of oils, source rocks, and tar sands in the Ardmore and Anadarko basins, in K. S. Johnson, ed., Anadarko Basin: 1988 Symposium Oklahoma Geological Survey Circular 90, p. 65–76.
- Pollastro, R. M., 2007, Total petroleum system assessment of

- undiscovered resources in the giant Barnett Shale continuous unconventional gas accumulation, Fort Worth Basin, Texas: AAPG Bulletin, v. 91, no. 4, p. 551–578, doi:[10.1306/06200606007](https://doi.org/10.1306/06200606007).
- Pollastro, R. M., D. M. Jarvie, R. J. Hill, and C. W. Adams, 2007, Geological framework of the Mississippian Barnett Shale, Barnett-Paleozoic total petroleum system, Bend arch–Fort Worth Basin, Texas: AAPG Bulletin, v. 91, no. 4, p. 405–436, doi:[10.1306/10300606008](https://doi.org/10.1306/10300606008).
- Portas, R., 2009, Characterization and origin of fracture patterns in the Woodford Shale in southeastern Oklahoma for application to exploration and development: M.S. thesis, University of Oklahoma, Norman, Oklahoma, 113 p.
- Schenk, C. J., 2005, Geologic definition of conventional and continuous accumulations in select U.S. basins: The 2001 approach (abs.)—2005 AAPG Hedberg Conference Understanding, Exploring and Developing Tight Gas Sands: AAPG Search and Discovery article 90042: http://www.searchanddiscovery.com/documents/abstracts/2005hedberg_vail/abstracts/short/schenk.htm (accessed September 16, 2009).
- Schmoker, J. W., 2002, Resource-assessment perspectives for unconventional gas systems: AAPG Bulletin, v. 86, no. 11, p. 1993–1999, doi:[10.1306/61EEDDDC-173E-11D7-8645000102C1865D](https://doi.org/10.1306/61EEDDDC-173E-11D7-8645000102C1865D).
- Schwarz, L., and A. Frimmel, 2004, Chemostratigraphy of the Posidonia Black Shale, southwest Germany: II. Assessment of extent and persistence of photic zone anoxia using aryl isoprenoids distributions: Chemical Geology, v. 206, p. 231–248, doi:[10.1016/j.chemgeo.2003.12.008](https://doi.org/10.1016/j.chemgeo.2003.12.008).
- Singh, P., 2008, Lithofacies and sequence-stratigraphic framework of the Barnett Shale, northeast Texas: Ph.D. dissertation, University of Oklahoma, Norman, Oklahoma, 181 p.
- Sinninghe Damsté, J. S., S. G. Wakeham, M. E. L. Kohnen, J. M. Hayes, and J. W. de Leeuw, 1993, A 6000-year sedimentary molecular record of chemocline excursions in the Black Sea: Nature, v. 362, p. 827–828, doi:[10.1038/362827a0](https://doi.org/10.1038/362827a0).
- Sinninghe Damsté, J. S., F. Kenig, M. P. Koopmans, J. Koster, S. Schouten, J. M. Hayes, and J. W. de Leeuw, 1995, Evidence for gammacerane as an indicator of water column stratification: Geochimica et Cosmochimica Acta, v. 59, p. 1895–1900, doi:[10.1016/0016-7037\(95\)00073-9](https://doi.org/10.1016/0016-7037(95)00073-9).
- Slatt, R. M., P. Singh, R. P. Philp, K. J. Marfurt, Y. Abousleiman, and N. R. O'Brien, 2009a, Workflow for stratigraphic characterization of unconventional gas shales: 2008 Society of Petroleum Engineers Shale Gas Production Conference, Fort Worth, Texas, SPE Paper 119891, p. 1–17.
- Slatt, R. M., P. Singh, R. P. Philp, K. J. Marfurt, Y. Abousleiman, N. R. O'Brien, and E. V. Eslinger, 2009b, Workflow for stratigraphic characterization of unconventional gas shales: Gulf Coast Association of Geological Transactions, v. 59, p. 699–710, doi:[10.2118/119891-MS](https://doi.org/10.2118/119891-MS).
- Slatt, R. M., P. Singh, R. P. Philp, A. Saison, Y. Abousleiman, N. R. O'Brien, and E. V. Eslinger, 2009c, Workflow for stratigraphic characterization of unconventional gas shales (abs.): Geological Society of America, Abstracts with Programs, v. 412, p. 12.
- Slatt, R. M., P. Singh, G. Borges, R. Perez, R. Portas, J. Vallejo, M. Ammerman, W. Coffey, and E. Eslinger, 2009d, Reservoir characterization of unconventional gas shales: Example from the Barnett Shale, Texas, U.S.A. (abs.): AAPG Search and Discovery article 30075: http://www.searchanddiscovery.com/documents/2009/30075slatt/ndx_slatt.pdf (accessed September 21, 2009).
- Slatt, R. M., et al., 2011, Outcrop/behind outcrop (quarry), multiscale characterization of the Woodford Gas Shale, Oklahoma (abs.): AAPG Search and Discovery article 80138: http://www.searchanddiscovery.com/documents/2011/80138slatt/ndx_slatt.pdf (accessed April 20, 2011).
- Sullivan, K. L., 1985, Organic facies variation of the Woodford Shale in western Oklahoma: Shale Shaker, v. 35, p. 76–89.
- ten Haven, H. L., M. Rohmer, J. Rullkötter, and P. Bissel, 1989, Tetrahymanol, the most likely precursor of gammacerane, occurs ubiquitously in marine sediments: Geochimica et Cosmochimica Acta, v. 53, p. 3073–3079, doi:[10.1016/0016-7037\(89\)90186-5](https://doi.org/10.1016/0016-7037(89)90186-5).
- Tissot, B. P., and D. H. Welte, 1978, Petroleum formation and occurrence: Berlin, Springer-Verlag, 538 p.
- Urban, J. B., 1960, Microfossils of the Woodford Shale Devonian of Oklahoma: M.S. thesis, University of Oklahoma, Norman, Oklahoma, 77 p.
- U.S. Geological Survey, 2009, Shale gas: http://energy.er.usgs.gov/gg/research/shale_gas.html (accessed September 16, 2009).
- Volkman, J. K., 1986, A review of sterol markers for marine and terrigenous organic matter: Organic Geochemistry, v. 9, p. 83–99, doi:[10.1016/0146-6380\(86\)90089-6](https://doi.org/10.1016/0146-6380(86)90089-6).
- Wang, D. H., and R. P. Philp, 1997, Geochemical study of potential source rocks and crude oils in the Anadarko Basin, Oklahoma: AAPG Bulletin, v. 81, no. 2, p. 249–275.
- Weston, R. J., R. P. Philp, and C. M. Sheppard, 1989, Sesquiterpanes, diterpanes and other higher terpanes in oils from the Taranaki Basin of New Zealand: Organic Geochemistry, v. 144, p. 405–421.
- Zhao, H., N. B. Givens, and B. Curtis, 2007, Thermal maturity of the Barnett Shale determined from well-log analysis: AAPG Bulletin, v. 91, no. 4, p. 535–549, doi:[10.1306/10270606060](https://doi.org/10.1306/10270606060).